

Hydrodynamics of plane liquid jets aimed at applications in paper manufacturing

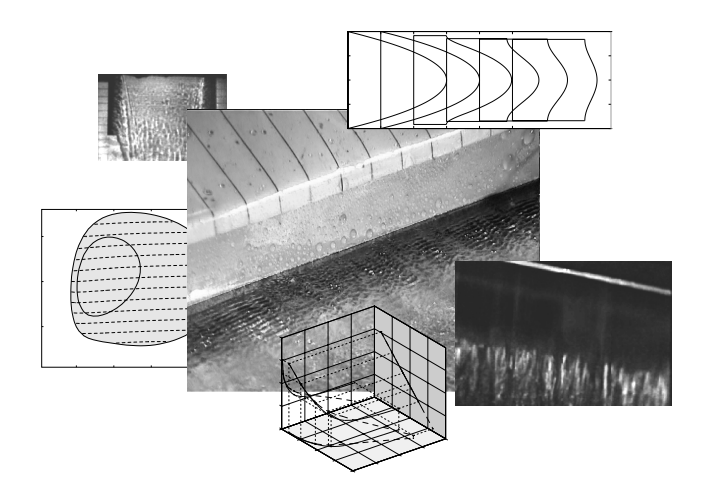
Daniel Söderberg

Doctoral Thesis Stockholm, 1999

Royal Institute of Technology
Department of Mechanics
FaxénLaboratoriet

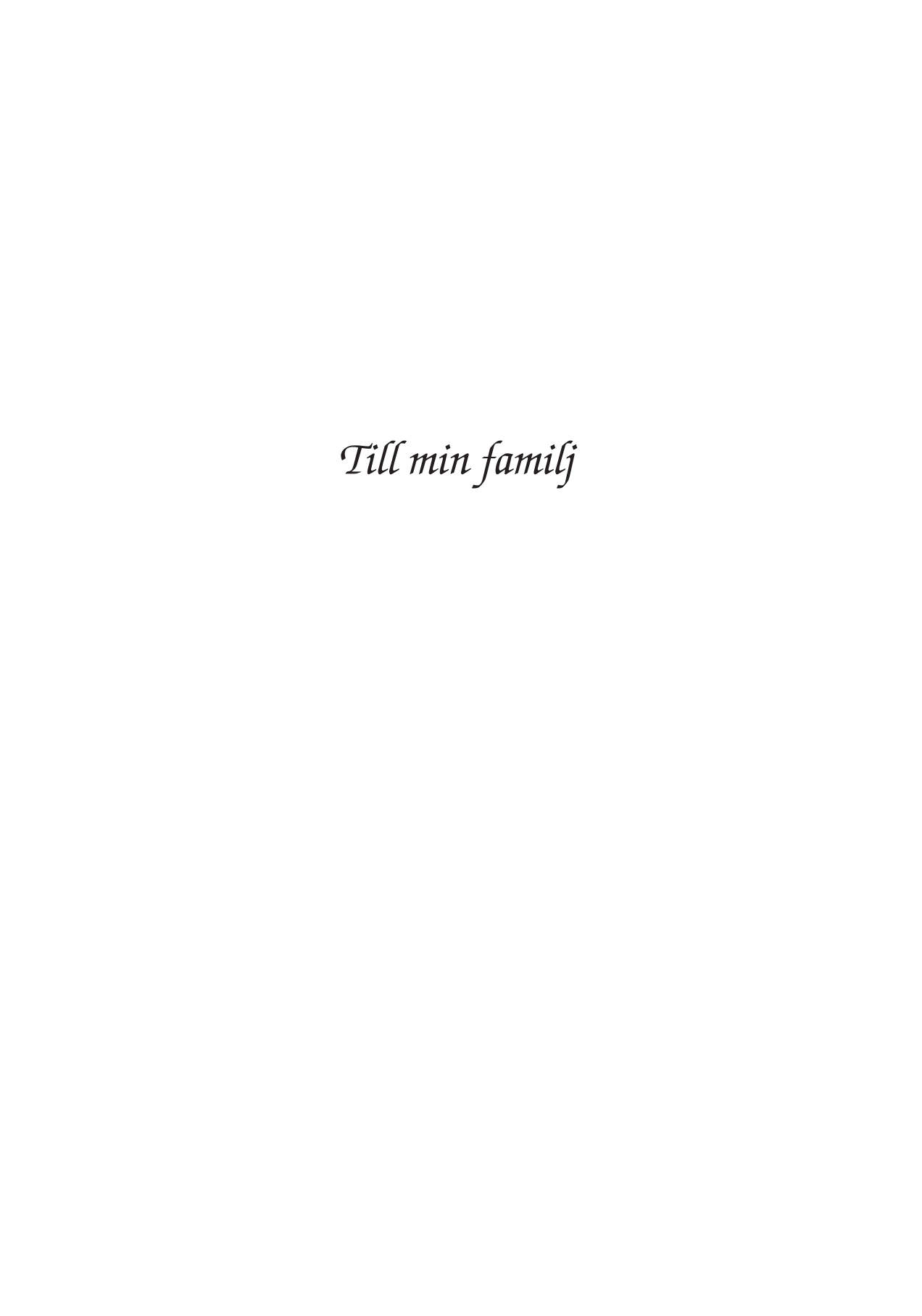
Hydrodynamics of plane liquid jets aimed at applications in paper manufacturing

by Daniel Söderberg



September 1999 Technical Reports from Royal Institute of Technology Department of Mechanics S-100 44 Stockholm, Sweden





Söderberg, D. 1999 Hydrodynamics of plane liquid jets aimed at applications in paper manufacturing

Department of Mechanics, FaxénLaboratoriet, Royal Institute of Technology S-100 44 Stockholm, Sweden

Abstract

Process industries are in general depending, in one way or the other, on fluid mechanics. Specifically, paper manufacturing, which probably is the dominant process industry in Sweden, is depending on the flow of cellulose fibres suspended in water. As a part of the process the suspension, consisting of fibres in water, is spread out on or between two moving permeable weaves, i.e. wires. The speed of this is usually 10–30 m/s and the suspension is spread out by a plane jet issuing from a headbox nozzle. It has been show that the conditions in the headbox and jet have a large influence on the quality of the final paper sheet. Primarily, streaks in the paper sheet are believed to be the result of streamwise streaks in the headbox jet.

The thesis is aimed at the flow phenomena which occur in the headbox jet. The investigations have been made with numerical calculations, stability theory and model experiments using water, as well as experiments with a real paper machine headbox and fibre suspension. In the thesis an introduction to the hydrodynamics of plane liquid jets is presented together with a description of the paper forming process and the fluid mechanics of headbox flow.

The basic flow and stability of a two-dimensional plane liquid jet has been investigated by numerical calculations, stability theory and experiments. The calculations of the laminar basic flow is successfully compared to pitot-tube measurements of the streamwise velocity profile. By visualisations of the flow it is found that wave disturbances on the jet has a severe effect on the flow. These waves can be predicted by linear stability theory, which shows the presence of five convectively unstable modes. These can be divided into three types and by comparison with the experiments the type of the visible waves is determined. These waves seem to initiate a break-up of the jet, which leads to strong streamwise streaks inside the jet.

By flow visualisation of headbox flow of an experimental paper machine, together with analysis of the resulting paper structure using the wavelet method the correspondence between flow disturbances and paper quality was investigated. It was shown that the wave instability, which is present on the low Reynolds number water jet, also can be found in the real the headbox jet. It is shown that these waves play an important role in the dynamics of the headbox jet and also have an influence on the final paper sheet.

Descriptors: liquid jet, transition, break-up, stability, wavelet, free surface, waves, streamwise streaks, fibre suspension, headbox, forming, shadowgraph, hot-film.

Preface

This thesis considers the hydrodynamics of plane liquid jets and specifically the flow of headbox jets within paper manufacturing.

- **Paper 1.** SÖDERBERG, L. D. & ALFREDSSON, P. H. 1998 Experimental and theoretical stability investigations of plane liquid jets. *Eur. J. Mech.* B/Fluids 17, 689–737.
- **Paper 2.** SÖDERBERG, L. D. & ALFREDSSON, P. H. 1999 Observation of streaky structures in a plane water jet. To appear in *J. Pulp Paper Science*.
- **Paper 3.** SÖDERBERG, L. D. 1999 A comparison between the flow from a paper machine headbox and a low Reynolds number water jet. In *Tappi Engineering Conference*, Septemper 12–17 1999, Anaheim, USA.
- **Paper 4.** SÖDERBERG, L. D. 1999 Absolute and convective instability of a relaxational plane liquid jet. To be submitted.
- **Paper 5.** SÖDERBERG, L. D. 1999 A visual study of the dynamics of a headbox jet. To be submitted.

Contents

Preface		vii
Chapte	r 1. Introduction	1
1.1.	Liquid jets	1
1.2.	Paper manufacturing	2
1.3.	The contents of this thesis	3
Chapte	r 2. Equations governing fluid flow	5
2.1.	Conservation of momentum and mass	5
2.2.	Navier-Stokes equations	6
2.3.	Hydrodynamic stability	8
Chapte	r 3. Hydrodynamics of liquid jets	16
3.1.	Steady flow of plane liquid jets	16
3.2.	Stability of plane liquid jets	19
Chapte	r 4. Paper forming	26
4.1.	Continuous forming	27
4.2.	Twin wire forming	28
4.3.	The headbox	29
4.4.	The fibre (pulp) suspension	30
4.5.	Cellulose fibres	32
Chapte	r 5. Fluid mechanics of headbox flow	34
5.1.	Manifold and tube bank	34
5.2.	Flow conditions in the nozzle	34
5.3.	Streak size in boundary layers and confined flows 36	
5.4.	Origin of streaks in headbox flow	37
5.5.	Influence of suspended fibres	39

x CONTENTS

5.6. Future Research	39
Chapter 6. Summary of Papers	40
Paper 1	40
Paper 2	41
Paper 3	41
Paper 4	42
Paper 5	43
Acknowledgments	44
References	45
Paper 1	51
Paper 2	113
Paper 3	129
Paper 4	155
Paper 5	185

CHAPTER 1

Introduction

Throughout history, fluid mechanics has served mankind in a vast amount of applications. In fact, life itself is very much dependent of the flow of many different fluids, e.g. water, air, blood and so on. Fluid mechanics has also served as a tool in human controlled processes at least since the invention of the spear. The spear, in contrast to e.g. a stone, has an aerodynamic design, which decreases air resistance and improves stability in flight. Another example is the boomerang. This knowledge was definitely a result of observations and extensive trials of features found in nature. As time passed tools and concepts, involving fluid mechanics phenomena, continued to evolve. This evolution was for a long time based on empirical knowledge.

Greek scientists, e.g. Aristoteles and Archimedes, were perhaps the first who introduced postulates on fluid flow. During the 18:th century experimental methodology and mathematical tools became available, which made it possible to extend the understanding of fluid mechanics. The technical topic which was driving the development was mainly aerodynamics. However, most process industries rely in one way or another on fluid mechanics in their manufacturing processes, although the awareness of this is often fairly low. But, in most cases tools and methods are the results of many years of trials and well suited for their task. In some cases, however, the fundamental concepts are not well understood and sometimes the tool or method is not optimised from a fluid mechanics point of view.

1.1. Liquid jets

The flow of a water jet into air is one of the most investigated phenomena in the early history of fluid mechanics and still today attracts a lot of attention. The initial interest was probably due to that liquid jets are common in everyday life and the flow is easy to observe. Leonardo DaVinci, for example, sketched the trajectory of jets discharging from orifices. Also, as one of the earliest quantitative results within fluid mechanics, Torricelli, deduced an empirical relation of the efflux rate through an orifice at the bottom of a container filled with water.

Plane liquid jets are used in several industrial applications. One of the primary reasons to investigate the flow of plane liquid jets has been to improve and control fuel atomisation. It has been shown that, in order to achieve atomisation, annular jets are more efficient than cylindrical jets. The annular jet can, if its thickness is small

1

2

compared to its diameter, be idealised as a plane liquid jet. Also, by having a coflowing high-speed gas jet the disintegration process can be improved further. This will, as the gas-fuel mixing is improved, increase the efficiency in e.g. jet engines. Coating is another industrial process, where plane liquid jets are used. In this case the uniformity of the jet is one of the most important issues. Also, within paper manufacturing and materials processing plane liquid jets play an important role.

1.2. Paper manufacturing

Paper manufacturing originates from China and is more than 2000 years old. The basic principle, on which the manufacturing is based, has however not changed. A suspension, which consists of water and some type of fibre, e.g. cellulose, is spread out on a permeable surface. The surface allows water to pass but traps the fibres. When the water is removed, the surface is covered with a thin paper sheet. The adhesion between fibres is a natural process governed by chemistry. Many things determine the properties of the sheet. Specifically the orientation of the paper fibres within the sheet depends on the flow as the fibres are forced to settle.

In modern paper manufacturing the formation of the paper sheet is a continuous process. The fibre suspension is formed into a plane liquid jet by a nozzle, which is called a headbox. The jet from the headbox lands on one or between two permeable weaves, which are called wires. It is obvious that the plane liquid jet plays an important part in the paper manufacturing process. The flow conditions in the headbox and jet are believed to have a major influence on the properties of the final paper sheet, see e.g. Norman (1996).

The way in which the flow field in the headbox and jet influences the paper sheet is not perfectly clear. Streaks oriented in the machine (streamwise) direction can in many cases be found in the final paper sheet. These streaks can be coherent variations in fibre orientation, formation or layer mixing in the case of layered forming. It has been shown that these streaks can originate from the headbox and jet. If this is the case, the streaks found in the paper sheet should be the consequence of some hydrodynamic feature in the headbox and/or jet.

Streaks and vortices are common in fluid flows. Hydrodynamics of Newtonian fluid flow suggests four possible origins of the streamwise streaks in a liquid jet, figure 1.1,

- Vortex stretching, which is a result of the accelerating flow, will give vortices aligned in the streamwise direction. This is a well-known mechanism and the origin of vorticity can for example be the upstream conditions in the nozzle, Aidun & Kovacs (1995).
- Centrifugal instabilities in the flow, which are caused by streamline curvature, see e.g. Matsson & Alfredsson (1990). This could be so-called Dean or Görtler vortices. The presence of this effect in the headbox was first proposed by Robertson & Mason (1961).

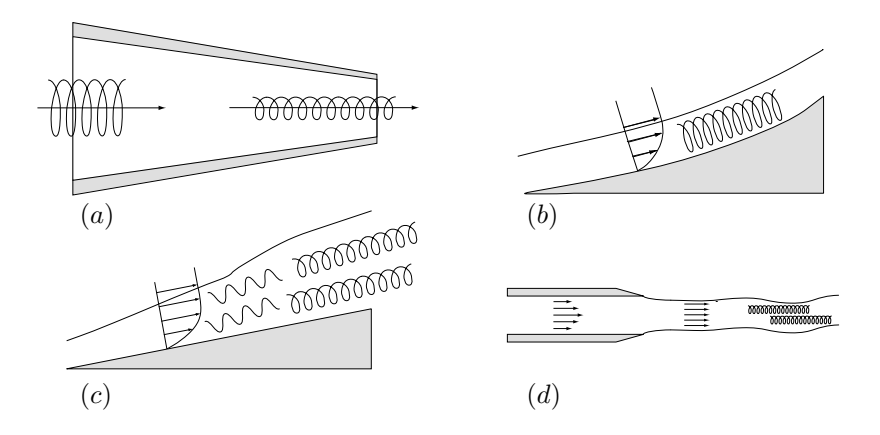


FIGURE 1.1. Streak creation mechanisms, which possibly could be present in headbox flow. (a) Vortex stretching, (b) centrifugal instability, (c) boundary layer transition and (d) wave instability.

- Streaky structures, which grow inside shear flows due to an algebraic instability could also occur at solid surfaces in the headbox, see e.g. Alfredsson & Matsubara (1996).
- Instability waves, which originate from velocity profile relaxation in the jet. The waves are found both for a plane water jet at low Reynolds numbers and in headbox flow. Coupled to these waves is a break-up of the jet, which generates dominating streamwise streaks.

The three first mechanisms are well known phenomena within fluid mechanics and the fourth was first observed by Söderberg & Alfredsson (1998).

1.3. The contents of this thesis

This thesis has been performed within the FaxénLaboratoriet, which is a *Centre of excellence* ("kompetenscentrum" in Swedish) initiated by the *Swedish National Board for Industrial and Technical Development* (Nutek). The centre is focused on fluid mechanics problems within various process industries. There are three main technology areas within FaxénLaboratoriet, Paper technology, Electro chemistry and Materials processing. Within the Paper technology group the work has been focused on the initial stage in paper forming, namely headbox flow and initial dewatering. A goal for the paper industry is to produce a paper which is homogeneous across its width (and length). The plane liquid jet emerging from the headbox in a typical paper machine has earlier been shown to be a possible source of observed non-uniformities in the final paper sheet.

4 1. INTRODUCTION

The present thesis is focused on the behaviour of plane liquid jets, both through basic theoretical/numerical and experimental studies of the stability of plane water jets, as well as direct measurements in a real paper machine. The measurements have mainly been through various types of flow visualisation of instability phenomena and these results have been compared with results from the stability analysis. The thesis is based on five separate papers, reporting various aspects of the research, as well as a general introduction and summary of the work. The present thesis gives in chapter 2 the equations governing the flow, including the boundary conditions, as well as some background regarding the stability of fluid flows. Chapter 3 gives an introduction to the hydrodynamics of liquid jets in general and in particular the stability of liquid jets. Chapter 4 gives an introduction to the modern technology of paper forming whereas chapter 5 gives details on the flow in headboxes. Chapter 6 summarises the five different papers which are included as appendices.

CHAPTER 2

Equations governing fluid flow

It is possible to formulate equations, which accurately describe many of the physical phenomena around us. In order for this to be possible a model has to be formulated, which describes the physics involved. The model can be either very simple, as Torricellis efflux formula, or very complex, as state of the art turbulence or rheology modelling. Common to all models is that they have limitations in validity. Within fluid mechanics the constant viscosity, non-elastic model of e.g. water or air suggested by Newton has been very successful. Even though equations can be formulated, it is seldom possible to obtain accurate/complete solutions except for idealised and/or simple flows. Today this has partly changed with the introduction of fast computers, which can solve the full set of equations numerically, i.e. Direct Numerical Simulations (DNS). Unfortunately there are still limitations on how complex problems it is possible to solve.

2.1. Conservation of momentum and mass

Fluid flow can be mathematically described with the momentum and continuity equations. These assure that there is a force balance within the fluid and that matter is conserved. In a Cartesian coordinate system this is formulated as

$$\rho\left(\frac{\partial u_i}{\partial t} + u_j \frac{\partial u_i}{\partial x_j}\right) = \frac{\partial \sigma_{ij}}{\partial x_j} + f_i, \quad i = 1, 2, 3$$
(2.1)

$$\frac{\partial u_j}{\partial x_j} = 0, (2.2)$$

Here (2.1) are the momentum equations (one for each spatial direction) and (2.2) is the continuity equation. Summation is assumed if two indices in a term are identical, i.e. Einsteins summation convention,

$$a_j b_j = \sum_{j=1}^3 a_j b_j = a_1 b_1 + a_2 b_2 + a_3 b_3.$$

In the equations $(u_1, u_2, u_3) = \vec{u} = (u, v, w)$ are velocities in the $(x_1, x_2, x_3) = \vec{x} = (x, y, z)$ directions respectively. Also, σ_{ij} is the stress tensor, f_i represents a body force and ρ is the density, which has been assumed to be constant. Another assumption is that the fluid is homogeneous. If, the fluid is a mixture of different phases (gas-solid,

solid-liquid or liquid-gas) or a mixture of fluids with different molecular structure this assumption can still be valid as long as the inter-phase structure of the mixture is smaller than a typical length-scale in the flow.

In the momentum equations σ_{ij} is the stress tensor, representing surface forces on a fluid element, which depend on the rate of strain (deformation) of the element. Hence, it is a function of the flow-field. Since incompressibility has been assumed the stress can be divided as

$$\sigma_{ij} = -p\delta_{ij} + \tau_{ij},\tag{2.3}$$

where p is the pressure and τ_{ij} is the deviatoric stress tensor. If τ_{ij} is neglected the flow is usually referred to as inviscid (perfect fluid). In order to solve for the fluid flow a model, which gives τ_{ij} as a function of the flow field, has to be formulated.

The behaviour of a fluid element under deformation yields a constitutive equation, which describes the relation between the stress in the fluid and the strain flow field, i.e. the rheology of the fluid. There exists a wide range of models to mimic the physics of different types of liquids, see e.g. Barnes *et al.* (1989). If the relation between stress and rate of strain is independent of direction the fluid is said to be isotropic and the, perhaps, most successful constitutive model for a fluid is an isotropic model, where the stress is linearly related to the rate of strain. Fluids obeying this relation, e.g. water and all gases, are called Newtonian fluids. Solutions to flows obtained with this model have shown to accurately mimic what can be observed experimentally.

If, for example, solid particles are added to a Newtonian fluid the linear relation may not hold (it depends on the volume concentration of particles). Instead a new model has to be deduced, which takes into account fluid-particle interaction etc. If the continuum assumption can be made, the flow of the suspension can be solved for by entering the new constitutive equation(s) into (2.3). If the continuum assumption is not fulfilled, a solution to the flow can still be obtained by solving the equations for the two phases separately. This can be done either with "one-way" coupling, i.e. the particles are transported by the fluid flow but do not affect the flow themselves. Or, it can be done with "two-way" coupling, where both the solid and fluid phases affect each other. It is easily understood that when the number of particles in the flow increases, the problem rapidly becomes too large to solve.

2.2. Navier-Stokes equations

If the fluid is Newtonian, the stress-strain relation gives a stress tensor τ_{ij} as

$$\tau_{ij} = \mu \left(\frac{\partial u_i}{\partial x_j} + \frac{\partial u_j}{\partial x_i} \right),\,$$

where μ is the dynamic viscosity. The governing equations (2.1) can then be recast into

$$\rho\left(\frac{\partial u_i}{\partial t} + u_j \frac{\partial u_i}{\partial x_j}\right) = -\frac{\partial p}{\partial x_i} + \mu \frac{\partial^2 u_i}{\partial x_k \partial x_k} + ge_i, \tag{2.4}$$

$$\frac{\partial u_i}{\partial x_i} = 0, (2.5)$$

which are called the Navier-Stokes equations. Here g is the gravitational acceleration and $\vec{e}=(e_1,e_2,e_3)$ its direction. As mentioned earlier, these equations can accurately describe the flow of water or air, as long as the density can be assumed to be constant. In order to solve the equations suitable boundary conditions have to be introduced. At solid surfaces the velocity will be zero,

$$u_i = 0, (2.6)$$

which usually is referred to as the no-slip condition.

If we have two phases, which do not mix, appropriate boundary conditions between them have to be implemented. An interface between the two phases is given by

$$F(\vec{x}, t) = 0,$$

which describes a surface in space. The kinematic equation describing the motion of the surface is given by

$$\frac{\partial F}{\partial t} + u_j \frac{\partial F}{\partial x_j} = 0. {(2.7)}$$

At an interface there has to be both a force balance and continuity of velocities (noslip), which can be expressed as

$$u_i^l = u_i^g, (2.8)$$

$$(\sigma_{ij}^l - \sigma_{ij}^g)n_j = s_i^\gamma, \tag{2.9}$$

where n_j is the normal to the interface, defined as positive in the direction from the liquid to the gas and $\sigma_{ij}^{l,g}$ is the stress tensors of the liquid (l) and gas (g) at the surface. Also, s_i is the force vector given by the surface tension and is defined as

$$s_i = \gamma \frac{\partial n_k}{\partial x_k} n_i,$$

where γ is the coefficient of surface tension and the normal to the surface can be obtained as

$$n_i = \frac{\partial F}{\partial x_i} / |\nabla F|, \quad |\nabla F| = \left(\frac{\partial F}{\partial x_k} \frac{\partial F}{\partial x_k}\right)^{\frac{1}{2}}.$$

These boundary conditions are general. If one of the phases constitutes a stationary solid boundary, the velocity condition (2.8) reduces to (2.6) and the surface tension is zero.

TABLE 1. Non-dimensional parameters.

$Re = \rho_l U_0 L / \mu_l$	Reynolds number
$We = \rho_l U_0^2 L / \gamma$	Weber number
$Fr = U_0/(Lg)^{\frac{1}{2}}$	Froude number
$\tilde{\rho} = \rho_g/\rho_l$	Density ratio
$\tilde{\mu} = \mu_g/\mu_l$	Viscosity ratio

For the case of a flow of a liquid and gas, both Newtonian, there will be 6 parameters (2 viscosities, 2 densities, surface tension and gravity) in the equations. By non-dimensionalisation with a suitable velocity U_0 and lengthscale L,

$$\tilde{x}_i = \frac{x_i}{L}, \quad \tilde{t} = \frac{tU_0}{L}, \quad \tilde{u}_i^{l,g} = \frac{u_i^{l,g}}{U_0}, \quad \text{and} \quad \tilde{p}^{l,g} = \frac{p^{l,g}}{\rho_{l,g}U_0^2},$$

the number of parameters may be reduced to five. These can be found in table 1. For a single-phase flow without the presence of gravity there will be only one parameter, namely the Reynolds number. This is the most widely used non-dimensional number within fluid mechanics and it has been shown that it is closely related to the stability of the flow.

2.3. Hydrodynamic stability

The transition from laminar to turbulent flow is (and has been) one of the main research areas within fluid mechanics today. If one considers the flow of a Newtonian fluid the occurrence of this transition process is strongly related to the Reynolds number, i.e. the relation between inertial and viscous forces. For low enough Reynolds numbers all flows (in an arbitrary geometry) will be laminar and at some stage, when the Reynolds number is increased, the flow will switch from laminar to turbulent. This does not imply that the flow becomes turbulent only as a consequence of the increase in the Reynolds number. In order to initiate a departure from the laminar state, there has to be a velocity field that promotes the growth of disturbances.

The evolution of disturbances with small amplitude in a laminar flow can be investigated by linearisation of the Navier-Stokes equations (2.4). This is done by the introduction of perturbations, which have the form $u_i = U_i + u_i'$ and p = P + p' into the equations. The basic flow field $(U_i$ and P) is assumed to be a solution to the equations and terms which are quadratic in the disturbance quantities are neglected. This gives equations, which describe the evolution of infinitesimal disturbances in a laminar flow.

If the flow field is basically two-dimensional, where the streamwise variation can be considered to be slow, the base flow can be assumed to be locally parallel, $U_i = (U(y), 0, 0)$. An example of such a flow-field is the laminar, zero-pressure gradient, boundary layer flow, see e.g. Schlichting (1979). The disturbance equations can then be reduced to

$$\left(\frac{\partial}{\partial t} + U\frac{\partial}{\partial x}\right)\nabla^2 v - D^2 U\frac{\partial v}{\partial x} = \frac{1}{Re}\nabla^4 v,$$
 (2.10a)

$$\left(\frac{\partial}{\partial t} + U\frac{\partial}{\partial x}\right)\eta + DU\frac{\partial v}{\partial z} = \frac{1}{Re}\nabla^2\eta,\tag{2.10b}$$

where the prime (') has been dropped, v is the disturbance velocity in the y-direction, D = d/dy and η is the normal vorticity defined as

$$\eta = \frac{\partial u}{\partial z} - \frac{\partial w}{\partial x}.$$

This formulation can be used to investigate the local behaviour of the laminar flow-field when subjected to a disturbance. Given the form of these two equations a normal mode ansatz can be made,

$$\{v'(y), \eta'(y), h'\} = \{\hat{v}(y), \hat{\eta}(y), \hat{h}\}e^{i\alpha x + i\beta z - i\omega t},$$
 (2.11)

where h' is the perturbation of the free surface, ω is the frequency, α and β are the streamwise and spanwise wavenumbers respectively. If this is inserted into (2.10) the result is,

$$(i\alpha U - i\omega)(D^2 - k^2)\hat{v} - i\alpha D^2 U\hat{v} = \frac{1}{Re}(D^2 - k^2)^2\hat{v},$$
 (2.12a)

$$(i\alpha U - i\omega)\hat{\eta} + \beta DU\hat{v} = \frac{1}{Re}(D^2 - k^2)\hat{\eta}, \qquad (2.12b)$$

where $k^2 = \alpha^2 + \beta^2$. These two equations are known as the Orr-Sommerfeld equation (2.12a) and the Squire equation (2.12b), respectively.

Also the boundary conditions (2.9) at a free surface have to be linearised. The surface is perturbed a distance h, figure 2.1, from its original location. The continuity of velocity at the surface (2.8), evaluated at the unperturbed location of the surface, gives,

$$u_i^l + hDU_i^l = u_i^g + hDU_i^g. (2.13)$$

Similarly for the stresses at the surface (2.9),

$$S_{ij}^{l}n_{j} + (\sigma_{ij}^{l} + hDS_{ij}^{l})N_{j} = S_{ij}^{g}n_{j} + (\sigma_{ij}^{g} + hDS_{ij}^{g})N_{j},$$
 (2.14)

where S_{ij} and N_j are the stress tensor and normal at the unperturbed surface location, respectively. If the flow is assumed to be locally parallel the equations can be rewritten

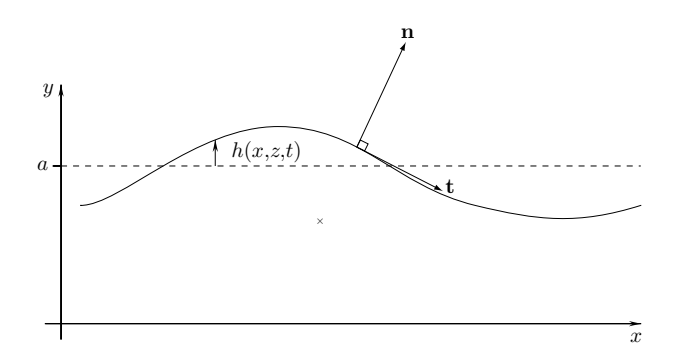


FIGURE 2.1. Definition of vectors on the free surface.

as

$$\begin{split} \hat{v}^l &= \hat{v}^g, \\ D\hat{v}^l - i\alpha\hat{h}DU^l &= D\hat{v}^g - i\alpha\hat{h}DU^g, \\ (D^2 + k^2)\hat{v}^l - i\alpha\hat{h}D^2U^l &= \tilde{\mu}\left\{(D^2 + k^2)\hat{v}^g - i\alpha\hat{h}D^2U^g\right\}, \\ (i\alpha U^l - i\omega)D\hat{v}^l - \frac{1}{Re^l}(D^2 - 3k^2)D\hat{v}^l - i\alpha DU^l\hat{v}^l &= \\ \tilde{\rho}(i\alpha U^g - i\omega)D\hat{v}^g - \frac{\tilde{\mu}}{Re^l}(D^2 - 3k^2)D\hat{v}^g - i\alpha\tilde{\rho}DU^g\hat{v}^g - \frac{ik^4}{We}\hat{h}. \end{split}$$

The procedure to obtain the conditions for the velocity at the surface is described in detail in Söderberg & Alfredsson (1998). The conditions for the vorticity are obtained in a similar manner,

$$\hat{\eta}^l + i\beta \hat{h}DU^l = \hat{\eta}^g + i\beta \hat{h}DU^g,$$

$$D\hat{\eta}^l + i\beta \hat{h}D^2U^l = D\hat{\eta}^g + i\beta \hat{h}D^2U^g.$$

The linearised equations and the appropriate boundary conditions constitute an eigenvalue problem,

$$\mathcal{D}(\alpha, \beta, \omega, Re, We)\{\hat{v}(y), \hat{\eta}(y), \hat{h}\} = 0, \tag{2.15}$$

where $\{\hat{v}(y), \hat{\eta}(y), \hat{h}\}$ are eigenfunctions and \mathcal{D} is a linear differential operator. In order for those to exist the dispersion relation,

$$\mathcal{D}(\alpha, \beta, \omega, Re, We) = 0, \tag{2.16}$$

has to be satisfied. This can be solved by fixing four of the parameters. The fifth is solved for and represents an eigenvalue. One such eigenvalue with corresponding eigenfunction is usually called a *mode*. Depending on the nature of the dispersion

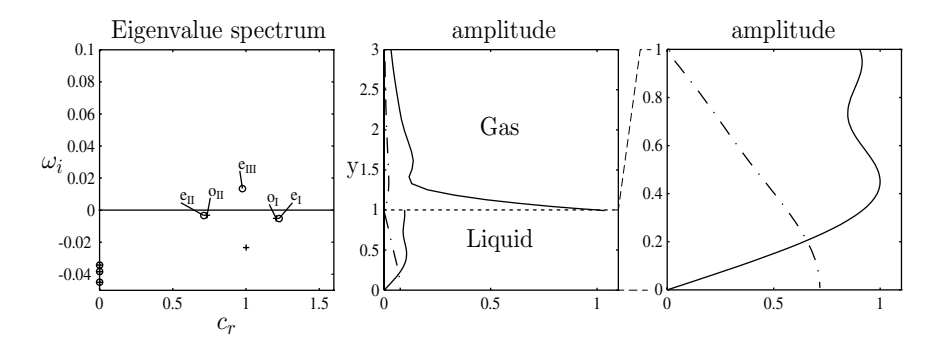


FIGURE 2.2. Eigenvalue spectrum (left), with one unstable even (sinuous) mode and the corresponding eigenfunction(s) in the gas and liquid (centre) and an enlargement of the liquid (right). In the graphs (\circ) is v-even and (+) v-odd modes. (-) u-amplitude and $(-\cdot -)$ v-amplitude. From Söderberg (1997).

relation a given set of parameters can give rise to one or more (even infinite) modes. This is usually referred to as an eigenvalue spectrum and an example can be seen in figure 2.2. This spectrum is obtained by solving for ω (α , β , Re and We fixed) and is taken from Söderberg (1997). It represents a position in the relaxational jet, where there are five unstable modes. The eigenvalues are complex and according to the normal mode ansatz, ω_r , corresponds to the frequency of the disturbance and ω_i to the growth or decay. The spectrum in this figure is plotted with the phase velocity c on the horizontal axis and the growth ω_i on the vertical axis. The phase velocity is defined as

$$c = \frac{\omega_r}{\alpha}$$

which represents the speed of a disturbance, i.e. the speed with which an individual wave-crest propagates. The normal mode formulation also gives that the disturbance grows if $\omega_i > 0$. Also, in the figure the eigenfunction in the gas and liquid corresponding to this eigenvalue can be found. The discontinuity of \hat{u} at the surface is an effect of the linearisation of the boundary conditions.

In this case the eigenvalue problem was formulated with real wavenumbers. The solution gave a complex ω and since $\omega_i>0$, the mode is growing in time. This formulation is usually referred to as temporal stability. If, on the other hand, the frequency is fixed, a solution can be sought for either α or β , which then will be complex. This is usually referred to as temporal stability. Most experiments concerning linear stability have been performed by initiating a periodic disturbance somewhere in the flow. The growth or decay has then been investigated as the disturbance travels downstream. This type of disturbances are referred to as convective, as it travels with the flow. The disturbance is then growing in space, hence spatial theory is consistent.

For a convective disturbance the frequency measured downstream of the forcing will always be constant, i.e. frequency locked. Another feature of convective instabilities is that when the forcing is removed, the disturbance will propagate away from the source and the flow will return to its unperturbed state.

2.3.2. The linear stability of a liquid column

One of the earliest results on the stability of a circular jet was obtained by Rayleigh (1896), who was able to predict the break-up of a circular liquid jet with a uniform velocity profile, see figure 2.3. Rayleigh chose a coordinate system moving with the liquid in the jet, i.e. the fluid is at rest. The steady jet, with radius a, is then perturbed and the energy potential of the free surface is studied. The perturbation has the form $R = a + \epsilon e^{i(\alpha x - \omega t)}$, where α and $\omega = \omega_r + i\omega_i$ are the wavenumber and angular frequency, respectively. The jet can be shown to be stable for all non-axisymmetric disturbances and the response to axisymmetric disturbances is given by

$$\tilde{\omega}^2 = \frac{\tilde{\alpha}I_1(\tilde{\alpha})}{I_0(\tilde{\alpha})}(\tilde{\alpha}^2 - 1),$$

where I_0 and I_1 are modified Bessel functions of the first kind and a non-dimensionalised frequency and wavenumber have been introduced such as,

$$\tilde{\omega} = \omega (\rho a^3 / \gamma)^{\frac{1}{2}}$$
 and $\tilde{\alpha} = \alpha a$.

This relation gives that

$$\tilde{\omega}^2 < 0$$
 for $0 < \tilde{\alpha} < 1$ and $\tilde{\omega}^2 > 0$ for $\tilde{\alpha} > 1$.

The disturbance is growing when $\omega_i>0$, which is obtained for $0<\tilde{\alpha}<1$. Hence disturbances grow when the wavelength is longer than the circumference of the jet. The growth rate for different wavenumbers can be seen in figure 2.3b. This was also the first success of what has come to be known as linear stability theory. The result showed an agreement with experimental results obtained earlier by Plateau (1873). Since surface tension is responsible for this instability of a free circular liquid jet, it is referred to as capillary instability and break-up. Even though the cylindrical liquid jet experiences a break-up it does not become turbulent, i.e. the loss of stability for a flow does not necessarily lead to turbulence. Later studies of the cylindrical jet has been performed both experimentally and numerically and is reviewed by McCarthy & Molloy (1974), Bogy (1979) and Debler & Yu (1988). Among other things it has been shown experimentally, Goedde & Yuen (1970), that non-linear effects cause ligaments between drops when the jet disintegrates. Also, it can be shown that the flow of a cylindrical liquid jet can be globally unstable, if proper boundary conditions are imposed at the upstream and downstream boundaries, Yakubenko (1997).

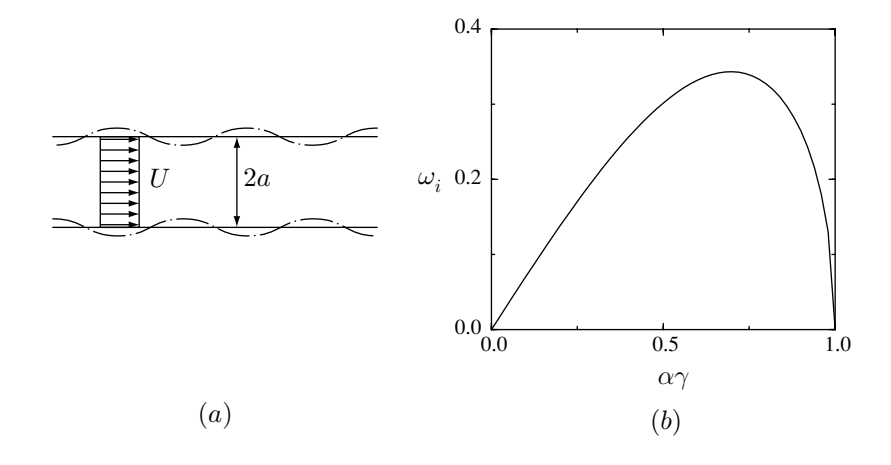


FIGURE 2.3. (a) Geometry of axisymmetric jet. (—) Rest state and (——) perturbed with an axisymmetric disturbance. (b) Growth ω_i as a function of the wavenumber.

2.3.3. Transition induced by linear instability

Linear stability theory has shown good agreement with experiments regarding the onset of many secondary flows and evolution of disturbances. One example is the so-called Tollmien-Schlichting (T-S) waves within a boundary layer on a flat plate, see e.g. Drazin & Reid (1981). By carefully performed measurements, where two-dimensional waves were initiated by a vibrating ribbon mounted on a flat plate perpendicular to the flow direction, the growth and decay of fixed frequency disturbances were found to be accurately predicted by linear theory, Klingmann *et al.* (1993). If, the T-S waves are growing and reach high enough amplitude they can initiate a breakdown and a subsequent transition to turbulence, see e.g. Henningson & Alfredsson (1996).

Another example is the curved channel flow, where streamwise vortices are formed as a consequence of centrifugal forces. This is usually called the Dean instability and is closely related to the Görtler instability found in flows over concave walls. The principle of these two types of flows can be found in figure 2.4. In both cases the streamlines are curved and thus a centrifugal force directed outwards (from a virtual origin) will act on a fluid element. A higher velocity will give a stronger force, which will give an unstable stratification. In some parameter regions this can be opposed by viscous forces or the radial pressure gradient, which also is an effect of streamline curvature. When instability sets in, streamwise stationary vortices are formed and these will be confined by the channel walls and boundary layer for the Dean and Görtler flow respectively. In figure 2.5 a series of images depicting a Dean flow can be seen. These images are taken from Matsson & Alfredsson (1990) and (from left to

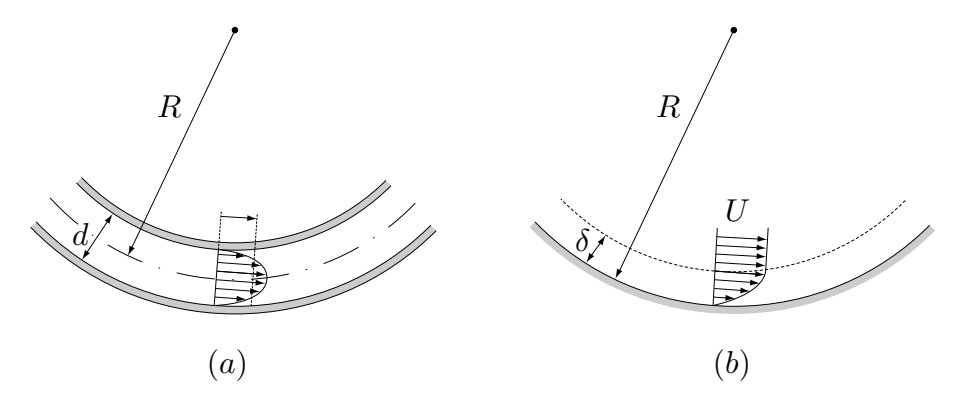


FIGURE 2.4. Centrifugal instability flows, (a) Dean and (b) Görtler.

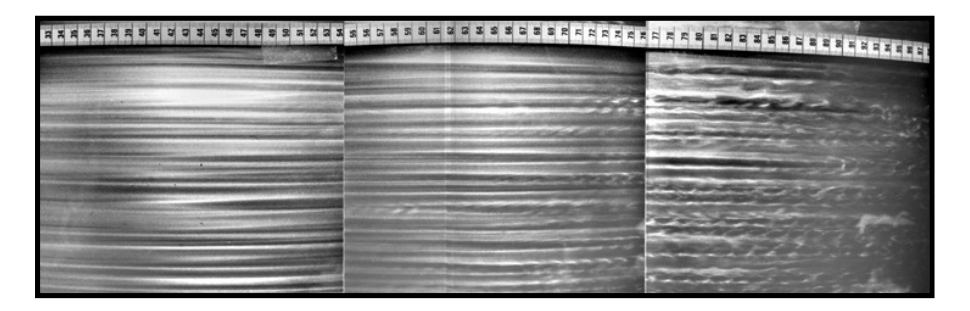


FIGURE 2.5. Curved channel flow, $Re=U_m d/\nu=960$, and d/R=0.025. From Matsson & Alfredsson (1990).

right) depicts the downstream development of the Dean instability. The visualisation is performed by adding reflective platelets particles to the flow. Initially well ordered vortices are visible with a spanwise periodicity of ≈ 1 cm, which is the same as the channel thickness. Downstream of this well ordered region travelling wave disturbances start to develop on the vortices. These waves are secondary disturbances, which grow downstream and finally may make the flow turbulent.

2.3.4. By-pass transition

It is well known that most wall bounded flows may undergo transition to turbulence at Reynolds numbers for which linear wave disturbances are stable. Such forms of transition are usually called by-pass transition, i.e. the TS-waves are not active (by-passed) in the transition scenario. Previously this has usually been associated with non-linear disturbances, however, there is also a possibility for a linear mechanism to initiate by-pass transition. The non-orthonormality of the eigenfunctions corresponding to the different eigenvalues introduce a possibility to obtain a transient growth



FIGURE 2.6. Smoke visualisation of streaks in the boundary-layer induced by free-stream turbulence. Flow is from right to left. From Matsubara *et al.* (1998)

of linear disturbances. The most amplified disturbance is usually a disturbance with $\alpha=0$, and such disturbances will initiate streaks in a shear layer. Even if the flow is stable (in the sense of infinitesimal wave disturbances) for all Reynolds numbers, as e.g. Hagen-Poiseuille or Couette flow, transient growth can still be possible. The growth is limited in time, whereafter viscous decay will occur. The growth of the streaky structures will not by themself give turbulence, but when they reach a certain amplitude secondary instabilities may develop which later breakdown into turbulence (Elofsson *et al.*, 1999).

The disturbance source which may induce a transiently growing disturbance can e.g. be free stream turbulence or wall roughness. Free stream turbulence is commonly occurring in confined flows and as the boundary-layer evolves, such disturbances will enter into the boundary layer, where they can set up streamwise elongated structures. This can be done continuously, as in the experiments by Westin *et al.* (1994) and Alfredsson & Matsubara (1996), or by creating localised controlled disturbances, see e.g. Westin *et al.* (1998). An example of this can be found in figure 2.6. This image is taken from a smoke visualisation of streaks in the boundary-layer induced by free-stream turbulence. The flow is from right to left and the streaks can be clearly seen. In the downstream end of the photograph some of the streaks can be seen to become wavy. This is a secondary instability and shortly after the appearance of the waviness, the streak breakdown to a turbulent spot.

CHAPTER 3

Hydrodynamics of liquid jets

Jets are created by the outflow of a gas or liquid through some kind of orifice or nozzle. The physical properties of the ambient media in comparison with the outflowing media will play a significant role in the behaviour of the jet. When a gas or liquid is ejected from a two-dimensional orifice into an ambient surrounding fluid with the same physical properties, the jet will rapidly spread due to the shear created by the velocity difference. The flow of an axisymmetric or plane laminar jet leaving a narrow orifice or slit can be solved with the laminar boundary layer equations and thus is only relevant for higher Reynolds numbers, see e.g Schlichting (1979). If the Reynolds number is higher the jet will become unstable and it will break down into a turbulent jet. This increase in diffusivity of momentum obtained with the transition to turbulence will enhance the spreading of the jet.

The big difference between free jets (gas into gas or liquid into liquid) and liquid jets emanating into a gas is the presence of a free surface. The liquid jet into air is bounded by a well-defined surface. The difference in density and viscosity of the two fluids is usually significant and thus at the lowest levels of assumption the presence of the surrounding gas phase can be ignored. If, however, there are irregularities on the surface (by e.g. turbulence within the liquid jet) there will be aerodynamic drag affecting the surface as well as the shear. Under some conditions the jet will disintegrate (atomisation).

3.1. Steady flow of plane liquid jets

A general geometry for the flow of a plane jet can be seen in figure 3.1. The jet is assumed to be homogeneous in the spanwise (z-axis) direction and it consists of liquid. It is ejected out of a converging channel and as the jet leaves the nozzle the noslip conditions (2.6) will change into the continuous velocity-force balance conditions (2.8) and (2.9). This will induce a relaxation towards a more uniform velocity profile further downstream. The liquid jet is surrounded by a viscous gas, which also has a velocity distribution. At a local position notation is used as in figure 3.1. In this figure the jet is assumed to be symmetric with respect to the centreline. The flow geometry is relatively simple, but the location of the free surface is unknown and has to be solved for, as well as the velocities and pressure.

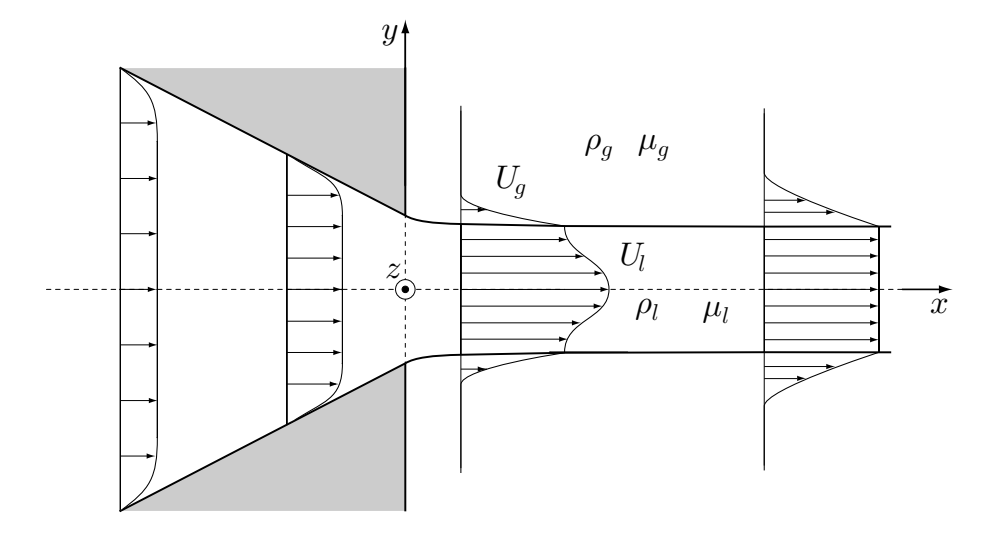


FIGURE 3.1. General geometry

As an application of the mathematical method of conformal mapping it is possible to calculate the flow field when the flow is assumed to be two-dimensional, inviscid and irrotational. Given those assumptions it is also possible to calculate free surface flows. This can for example be done for the outflow of a liquid jet through an orifice (slit), see e.g. Lamb (1932) or Pai (1954). An extension to nozzles with arbitrary contraction angle can also be made, Söderberg (1994). Liquid sheets do not necessarily have to be created by nozzles, but can also be created by two jets, which impinge against each other, Taylor (1960). Even if a plane liquid jet is ejected from a nozzle with a rectangular exit, it will change shape due to the effects of surface tension, see Taylor (1959b). At the sides of the jet there will be a rim with high surface curvature, which will cause a pressure difference between the surrounding air and the liquid in the rim. This will give a spanwise contraction of the jet and an example of this can be seen in figure 3.2.

The contraction can be prevented by introducing guiding wires attached to the spanwise sides of the nozzle. This was done in an experimental investigation of the plane liquid jet flow at low Reynolds number, Brown (1961). The aim of this investigation was to improve a coating process. The plane jet was issued vertically and onto a rotating cylinder in order to mimic the coating process. As one of the results of this investigation, the flow of the air at the impact line on the cylinder showed to be important. If it was allowed to flow freely (induced by the rotating cylinder and viscosity) it could enter between the liquid and the surface of the cylinder, which would give a distorted contact line. However, if the air flow was blocked immediately before the impact line this could be prevented.

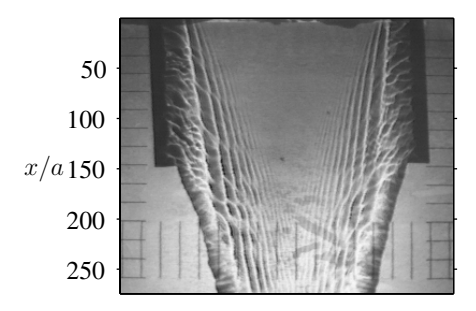


FIGURE 3.2. Photograph of a plane water jet at 1.3 m/s. The width of the jet is 15 cm and the thickness is 1.1 mm. The jet exhibits a spanwise contraction and at the sides of the jet the free rims are visible.

The case of a laminar viscous liquid jet flowing out of a channel with an initially fully developed parabolic velocity profile was solved by Lienhard (1968) with an approximate method, which included both gravity and surface tension. Also, a solution was obtained by Tillet (1968), who used the boundary layer equations. Yu & Liu (1992) numerically solved the flow of a laminar plane liquid jet emanating from a nozzle with varying contraction ratio (converging angle) of the nozzle. The results show that the thickness of the plane liquid jet increases when it leaves the nozzle for low Reynolds numbers, $Re = \mathcal{O}(10)$, i.e. die-swell (see Joseph, 1978). If the contraction ratio is increased, the expansion becomes smaller and when the Reynolds number is increased a high contraction ratio gives a location of the surface as predicted by the theory for a potential jet.

In the scope of these results one may ask the question: Under which circumstances does one obtain a (close to) potential flow as shown by Yu & Liu (1992)? A contracting channel (nozzle) will decrease the boundary-layer thickness at the walls due to the acceleration of the flow. The solution to the laminar flow in a converging channel can both be obtained by the boundary layer equations, e.g. Falkner-Skan and Polhausens solution, or it can be solved exactly, i.e. the so-called Jeffrey-Hamel solutions for diverging and converging channels. In figure 3.3 the nozzle edges are positioned at x=a. The boundary layer thickness, δ , at this position would then be $\delta=3a(Re)^{-\frac{1}{2}}$. At Re=1000 this gives $\delta\approx a/10$, which means that the effect of viscosity is limited to a region close to the wall. Also, potential flow theory indicates a higher velocity at the surfaces of the jet as it leaves the nozzle, which would reduce the boundary layers further.

Due to the rapid increase in computing power, it is today relatively simple to solve two-dimensional laminar flows numerically. However, the flow of a two-dimensional plane liquid jet poses some extra difficulties. If, the solution of the location of the

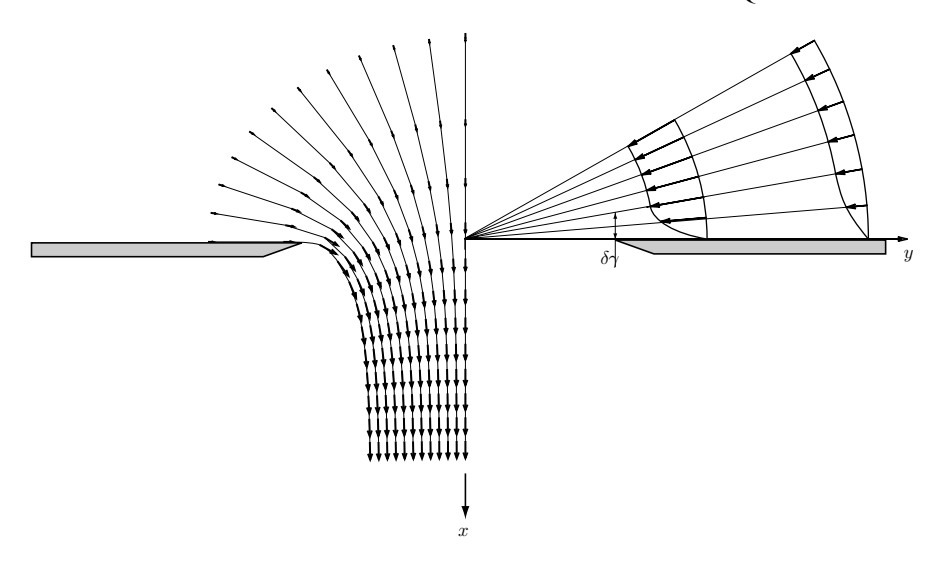


FIGURE 3.3. Potential flow through a slit calculated by conformal mapping (left) and boundary layer evolution in a converging channel (right). The velocity is represented by vectors and the streamlines are also shown.

free surfaces should be obtained accurately, some algorithm has to be implemented in order to track them. This is especially important if surface tension is included in the problem formulation. Goodwin & Schowalter (1995) solved the flow with inclusion of gravity and surface tension. They calculated the flow for situations where the effect of gravity and surface tension was high and the jet is directed almost vertically upwards, which causes severe bending of the jet.

Numerical solutions for the high Reynolds number flow of a two-dimensional laminar jet leaving a finite length channel were performed by Söderberg & Alfredsson (1998). The calculations were compared to pitot-tube measurements in a plane water jet. This showed a fair agreement, see figure 3.4. The figure shows an almost parabolic velocity profile at the channel exit and as the liquid leaves the channel there is a relaxation towards a uniform profile downstream. A scaling of the streamwise distance from the nozzle with the Reynolds number, x/Re, shows a strong similarity of the flow for higher Re, figure 3.5. In the figure the centreline and surface velocities are plotted as well as the location of the free boundary.

3.2. Stability of plane liquid jets

It is clear that the steady flow of a plane liquid jet can be disrupted. From the result for the circular jet, section 2.3.2, it was clear that surface tension can have a de-stabilising effect. Which are the phenomena occurring in a plane liquid jet and what effects can

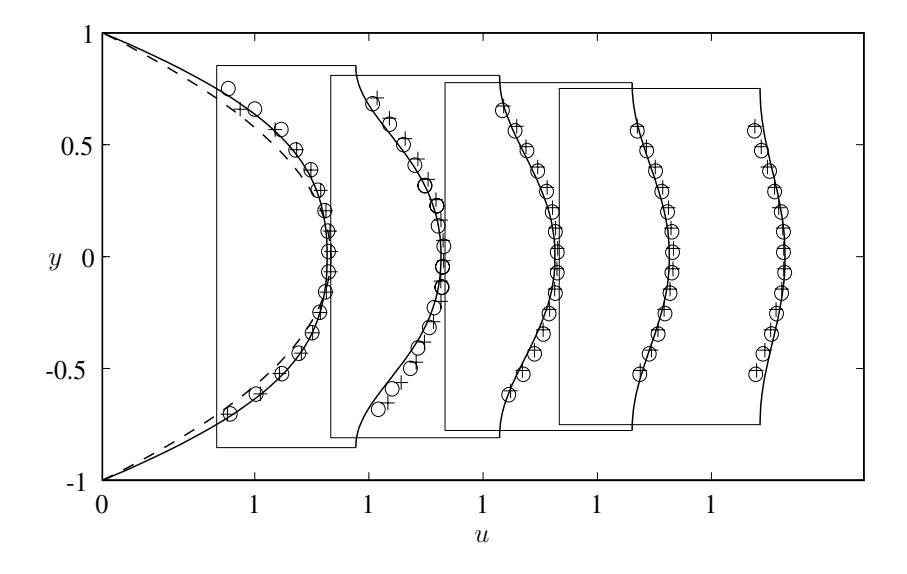


FIGURE 3.4. Velocity distribution in the channel jet. (—) calculated, (+) and (o) measured, (– –) parabolic profile with the same maximum velocity as the measured profile. $U_m=1.3~\mathrm{m/s},$ $a=0.55~\mathrm{mm},$ Re=700 and We=12.5, profiles at $x=0,10,20,30,40~\mathrm{mm}.$

be seen? Squire (1953) made an analysis of a liquid sheet with identical assumptions to Rayleigh (1896) for the liquid cylinder. The result clearly showed that it was linearly stable to all perturbations since, for this case, surface tension will act as a stabilising force.

Dombrowski & Fraser (1954) performed experiments with plane liquid jets related to atomisation applications. The investigation studied the effects of nozzle design. The experiments clearly showed the presence and downstream growth of sinuous disturbances. Those had a wavelength significantly larger than the typical sheet thickness.

In order to directly explain the observations of unstable plane jets, Hagerty & Shea (1955), introduced an inviscid stagnant gas in the analysis. When this is done there is nothing to gain by transforming into a coordinate system that travels with the liquid velocity. As a part of the result, they were able to show that the only existing solutions were symmetric or anti-symmetric. These two types of modes can be seen in figure 3.6 and can also be referred to as dilatational or sinuous respectively. The dispersion relations they obtained gave that the jet can be unstable in a certain parameter range. It was also found that the sinuous disturbance always is the most amplified. The mechanism, which causes this instability, is the drag induced on the travelling waves

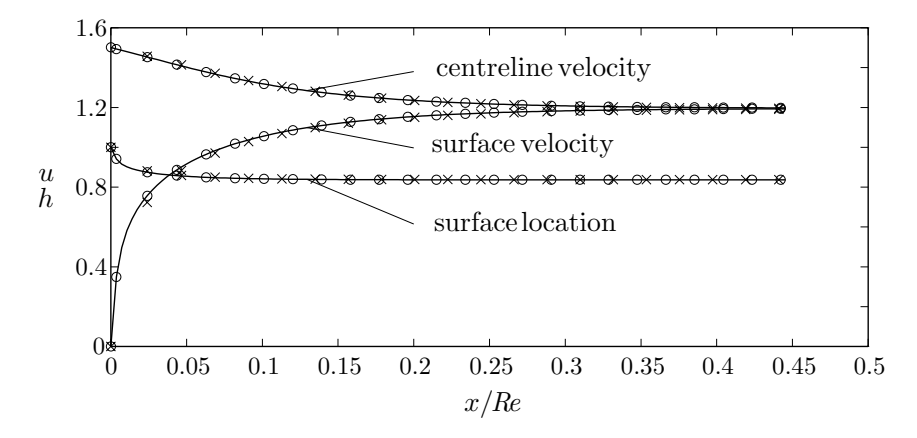


FIGURE 3.5. Velocity at the centreline and surface as well as the location of the free surface. (×) Re = 100, (o) Re = 1000; (—) Re = 10000, $\tilde{\rho} = 0$ and $\tilde{\mu} = 0$.

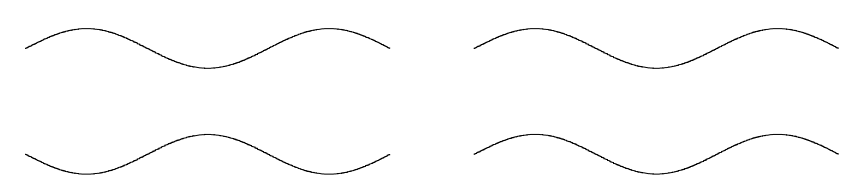


FIGURE 3.6. Definition of symmetry. Symmetric or varicose (left) and antisymmetric or sinuous (right).

by the surrounding gas, i.e. the instability has aerodynamic origin. They also made simple experiments, which were compared to the theory with a fair agreement.

A more careful experimental investigation was performed by Taylor (1959a), in which a radially spreading sheet was studied, both by direct visualisation and by the Schlieren method. In the investigation point disturbances were introduced and the result studied. It was found that both sinuous and dilatational disturbances were present in the sheet. Dilatational waves are dispersive and propagates more slowly than the sinuous waves. The disintegration of liquid sheets was also studied by Taylor (1959b).

Brown (1961) disturbed the plane liquid jet and investigated the Weber number dependence for propagating waves in/on the jet. It was found that the waves only propagated upstream if We < 1. By considering a viscous liquid sheet with the presence of surface tension Lin (1981), with linear stability theory, showed that the only amplified disturbance are a spatially growing wave with negative group velocity $c_g < 0$, i.e. it is propagating upstream. This was found to occur only when We < 1, which is in complete agreement with the experimental result. The result was obtained under the assumption that the sheet is thin. The agreement between experiment and

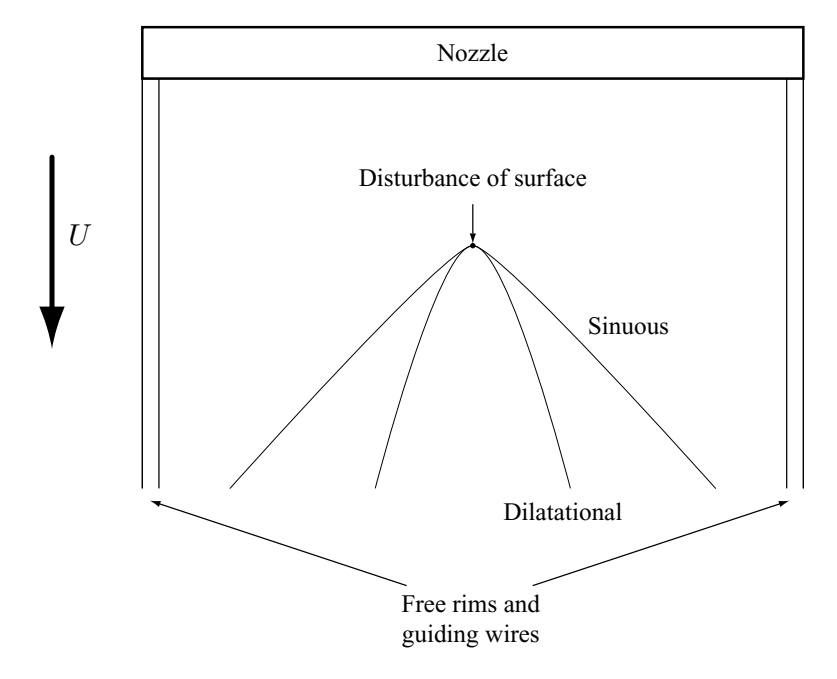


FIGURE 3.7. The observed wave pattern by introducing a disturbance at the surface.

theory was also shown in the experiments by Lin & Roberts (1981), the sheet was disrupted by placing an obstacle through it, which forces the sheet to split and form a Λ -shape with the tip at the obstacle. This gives rise to both sinuous and dilatational waves as depicted in figure 3.7, and both patterns are is in agreement with theory.

In order to refine the analysis and investigate the break-up and atomisation of a plane liquid jet Lin, Lian & Creighton (1990) and Li & Tankin (1991) refined the analysis with an assumption of a viscous liquid and an inviscid gas. Their investigations yielded identical dispersion relations, which were studied in different parameter regions. It was found that instability is promoted by the aerodynamic drag and in a certain parameter region viscosity is enhancing the instability.

Lin et al. (1990) found that the sheet was absolutely unstable for sinuous disturbances with We < 1 independent of Re and $\tilde{\rho}$. If We > 1 it is stable if the density ratio, $\tilde{\rho}$, is zero and otherwise convectively unstable. The dilatational mode always has a region of convective instability except for $\tilde{\rho} = 0$. The instability is of capillary origin for We < 1 otherwise the instability arises as a result of the pressure fluctuation at the surface.

Up to this point, the models studied made it possible to obtain implicit dispersion relations. If the velocity in the gas and liquid departs from uniform the solution

has to be found numerically by solving the eigenvalue problem arising from the Orr-Sommerfeld equations (2.12a).

By solving the eigenvalue problem of a viscous liquid sheet in a viscous gas Teng, Lin & Chen (1997) refined the analysis. The velocity field in the sheet is slightly modified for this case due to the shear exerted on the surface by the surrounding gas. The problem was solved using a spectral method. It was shown that absolute instability is caused by surface tension and convective instability by the velocity difference. Also, an increase of $\tilde{\rho}$ enhances instability.

Earlier, an investigation of the stability of a relaxational liquid jet was performed by Hashimoto & Suzuki (1991), where velocity profiles were calculated with the approximate method of Lienhard (1968). They solved the temporal stability problem using a shooting method disregarding the ambient air. They identified four unstable modes, two sinuous and two dilatational. The calculations were performed in order to explain the presence of two-dimensional spanwise homogeneous travelling waves, which they found in experiments. The comparison between experiments and theory showed a fair agreement with the stability calculations, when the observed wavenumber variation in the streamwise direction was compared with the location of maximum growth. However, their calculation, with which they compare the experimental results, does not include surface tension and they later showed that surface tension has a considerable effect on both growth rate and phase speed. Also, the flow is spatially varying and a convective disturbance should be frequency locked in this flow situation (i.e. the frequency should be constant). Hence wavenumber variation will not follow the maximum growth ridge in the plane given by the parameters α and x/Re.

The small waves identified by Hashimoto & Suzuki (1991) resemble the experimental results obtained for a cylindrical liquid jet by Hoyt & Taylor (1977). The wavelengths found for this case were compared with linear stability results by Brennen (1970), which were obtained for a hydrodynamic cavity behind axisymmetric objects.

A similar investigation was performed by Söderberg & Alfredsson (1998). The base flow was in this case calculated directly from the two-dimensional equations. The eigenvalue problem was solved using a spectral method. The result clearly showed the presence of a fifth unstable mode (sinuous). In their experiments, naturally occurring waves were found on the jet without forcing above a certain critical velocity. Also, waves could be forced using acoustic excitation, which made it possible to measure the amplitude function of the disturbance throughout the jet. A comparison was made between wavenumber variations in the jet obtained with image processing and results from the stability calculations. The stability formulation was temporal, hence the result is not clear-cut, but a transformation was used to make the comparison. The agreement was only modest.

Söderberg (1999a) improved the analysis by solving the spatial stability problem and comparing them to experimental results regarding wavenumber variations and

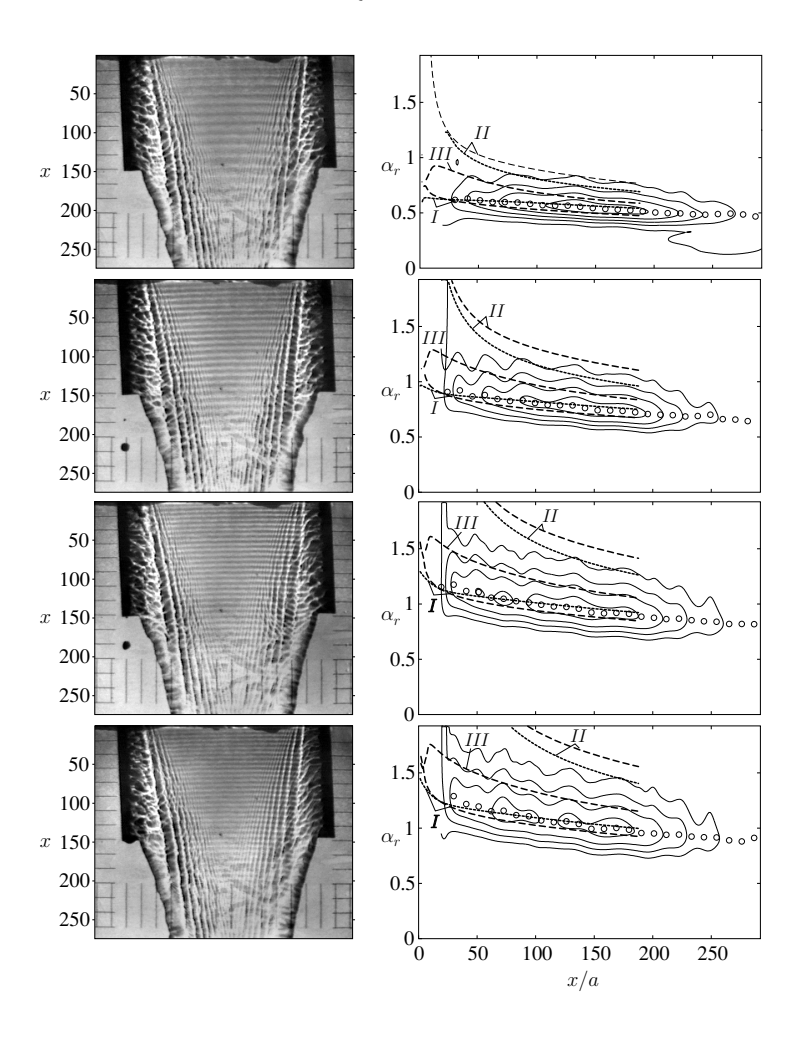


FIGURE 3.8. Comparison between experimental and theoretical results regarding wavenumber variation, from top to bottom f=340, 485, 612, 669 (Hz). Re=700, We=12.5 and a=0.55 mm. Sample images with forced wave disturbances (left) and results from wavelet transform and theory (right). In the contour plot the experimental maximum is marked (\circ) and wavenumber variation from spatial stability theory is marked both for sinuous (--) and dilatational (\cdots) modes. The contour spacing is 10% of the maximum level. The type of mode is indicated in the graphs (I, II and III)

spatial growth. An example can be seen in figure 3.8. This figure shows the wavenumber variation for four different forcing frequencies. The contour plots (right column) represents the solution from a wavelet analysis of a series images (left column) taken by a CCD-video camera. The contours represents levels of constant amplitude of the continuous Morlet-wavelet convolution (Farge, 1992). In each graph the wavenumber is plotted as a function of the non-dimensional x-coordinate. The wavenumber variation for the five most unstable modes are plotted on top of the wavelet transform map. It is, from these graphs, possible to conclude that the observed waves initiated by acoustic forcing are of type I (cf. figure 2.2). For the four frequencies the wavenumber is decreasing downstream in the jet. Also, a higher frequency gives a higher wavenumber. The modes of type I have the lowest wavenumber, which is roughly one-half of modes II. In between those two pairs the fifth (sinuous) unstable mode, III, can be found.

CHAPTER 4

Paper forming

The principle of paper manufacturing was known already by the Chinese two thousand years ago. The basic components used to produce a paper sheet are cellulose fibres and water. Here the secret of paper production prevails. Cellulose fibres dissolved in water do not bond, but as water is removed, chemical bonds form naturally between the fibres. The Chinese made the paper by handsheet forming. The principle can be seen in figure 4.1. A mix of water and fibres are put on top of a permeable surface (wire) and due to the gravitational force water passes through the wire whilst the fibres are trapped. Thus a sheet is formed at the permeable surface. The de-hydration of the fibre mat can be continued by pressing the fibre mat between two blankets (felts). Finally the sheet is allowed to dry by evaporation of water. The properties of the final paper sheet are a function of the fibre properties and the method used to produce the paper.

There are many factors influencing the sheet but the forming plays an essential role. The way that fibres can be affected at this stage is mainly by hydrodynamic forces acting on the fibres in the suspension. Based on the conditions in the flow field, the interaction can be either through viscous forces (friction) or inertial forces (drag). At the time when the fibre suspension is put on the wire any kind of applied forcing, in this case horizontal shaking, will influence the way in which fibres are layered in the mat.

The method of hand forming of paper sheets is not very quick. The initial drainage of water is driven by gravity. Initially, water passes through the permeable wire surface without any additional resistance. But, as this takes place fibres are transported by the flow towards the holes in the surface where they are trapped. This settling of fibres takes place as long as there is a flow through the fibre mat, which builds up on the wire. Cellulose fibres have a higher density than water and can therefore also settle by sedimentation. However, this is not the settling mechanism used in paper forming.

It is also clear that this forced settling of fibres introduces a self-healing effect in the sheet, i.e. at points where there are less fibres the flow will increase (due to local decrease of flow resistance) and thus the transport of fibres to that point will increase. This principle is illustrated in figure 4.1. In (a) dewatering has just started, and since the permeability of the wire is constant, dewatering will be uniform. As this proceeds, (b), fibres are convected with the flow towards the holes in the sheet. Due to the initial position of fibres in the suspension some holes in the wire are blocked

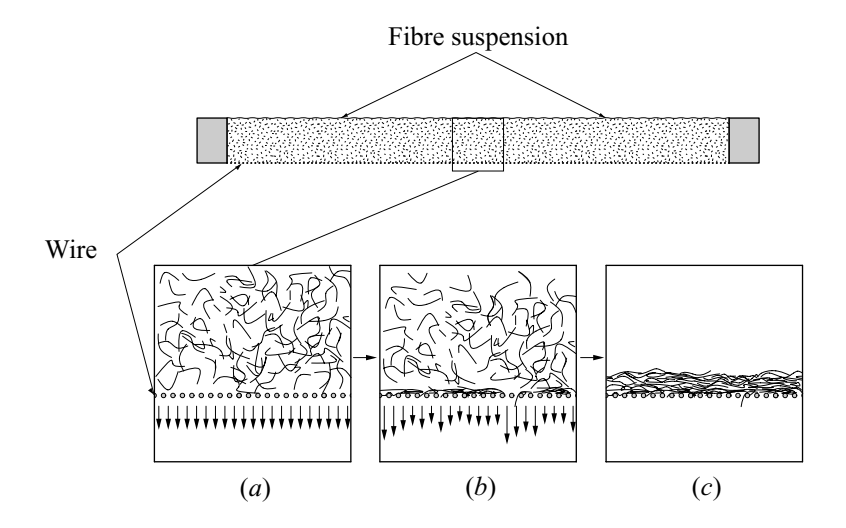


FIGURE 4.1. Principles of hand sheet forming

more than others, which generates an increase in flow towards the positions on the wire where permeability is higher. Thus more fibres are convected towards the high-permeability regions. The final fibre mat (c) is then more uniform than it would be if the self-healing effect was not present. This implies that a sheet with randomly positioned fibres always will have a higher variation of local sheet grammage¹ than the real (formed) sheet. Only as the sheet becomes infinitely thick, the variation in a random sheet will approach the lower variation in a formed sheet. The self-healing effect was discussed by Wrist (1961) and has later been shown by simulation and experimentally by Haglund $et\ al.\ (1974)$.

4.1. Continuous forming

The handsheet forming method described in the previous section is a tedious process. To increase production a continuous method was invented by the Frenchman Nicholas Louis Robert in 1798. In figure 4.2 the principle of this paper machine can be seen. The fibre suspension is distributed on top of an endless wire (a). Dewatering initially takes place due to gravity (b) after which the fibre mat is pressed (c) and rolled up (d). Final drying is performed separately, i.e. offline. In 1807 the Fourdrinier brothers, with assistance of an engineer Bryan Donkin, built a bigger and further improved machine. This type of paper machine is today called "fourdrinier" machines. This continuous process including drying, resulted in an increased production of paper, but the possibility to control the initial stage of dewatering decreased. When paper sheets

¹Grammage is the weight per unit area, i.e. it has the dimension $[kg/m^2]$. This is usually denoted w.

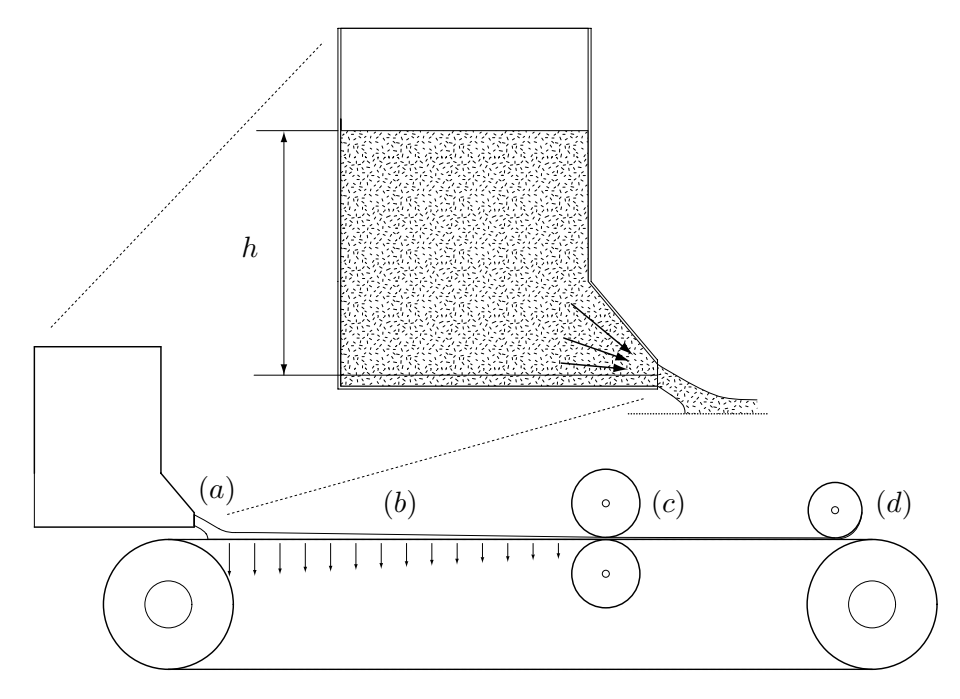


FIGURE 4.2. Robert principle of single wire forming, (a) initial forming, (b) dewatering, (c) pressing and (d) roll up of paper.

are formed by hand the human influence should not be underestimated and there exists today no machine with the same possibilities to adaptively control the process. One property, which is common between the early hand making of paper and the one-sided continuous dewatering principle, is the asymmetry of the final paper sheet. This is a consequence of the one-sided dewatering of the web.

However, the continuous forming method (single wire) has improved since these first machines. The basis for the improvement has mainly been empirical. The insight in the mechanisms, which control the forming of the sheet on the wire, has been limited. Fourdrinier machines are still widely used in paper manufacturing. In order to control the sheet properties the draining fibre suspension can today be subjected to different degrees of vertical agitation.

4.2. Twin wire forming

In the 1950's experiments were performed where the fibre suspension was introduced between two wires, which can be seen in figure 4.3. The main aim was to improve the dewatering capacity. In fact, the introduction of two wires did not double the dewatering capacity but rather quadrupled it. This is a result of water being removed at two sides and reduced dewatering resistance since the fibre mats are only half of that

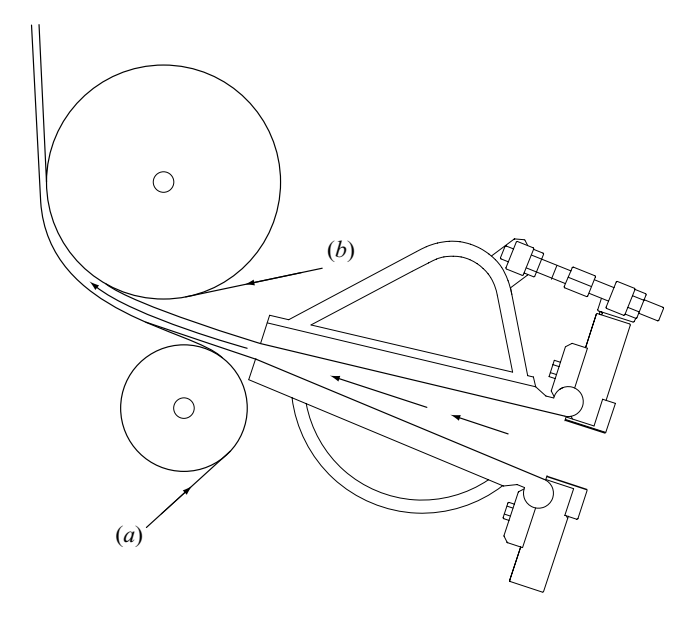


FIGURE 4.3. Principles of twin-wire roll forming, (a) tensioned outer wire, (b) Inner wire.

in single sided dewatering. The principle shown in figure 4.3 is called roll-forming and dewatering pressure, δp , is obtained as

$$\delta p = \frac{T}{R},$$

where T is the outer wire tension and R is the radius of the roll. The dewatering can also be initiated by letting the wires pass between blades mounted in a staggered pattern on both sides of the wires. The blades are pressed onto the wires, which generates a dewatering pressure. This is usually referred to as blade-forming.

An increase in dewatering capacity allows for higher machine speeds and the introduction of twin-wire forming introduced a method, where the final paper sheet can be more symmetric.

4.3. The headbox

The fourdrinier machine used an open headbox mounted on top of the forming table, figure 4.2. At the bottom of the headbox a slit allowed the fibre suspension to be continuously delivered on top of the wire. The speed of the jet was controlled by the height of the water in the headbox. A higher water column gives a higher velocity, i.e. the same principle as was first investigated by Torricelli for a circular orifice. To increase speed the height of the water has to be increased. If viscous effects are

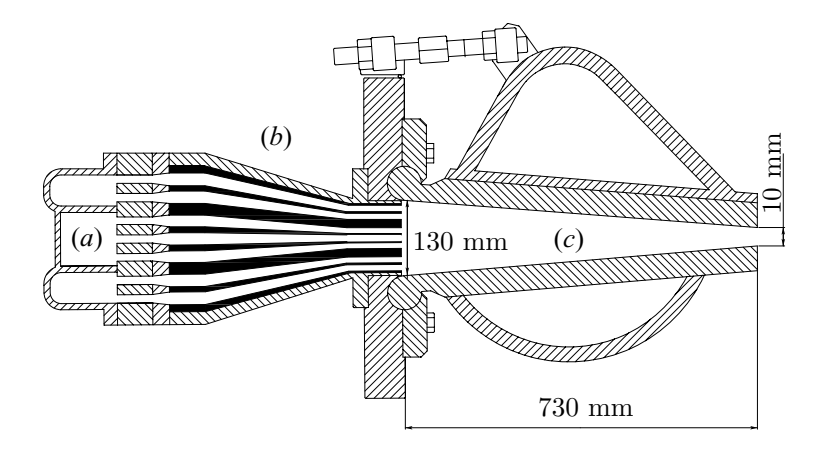


FIGURE 4.4. A modern headbox design. (a) Manifold channel, (b) tube package and (c) nozzle.

ignored the jet speed, U, is given by the Bernoulli equation,

$$U = (2gh)^{\frac{1}{2}},$$

where g is the gravitational acceleration and h is the water height. It is obvious that if the speed is doubled, the water level has to be be four times higher, e.g. to get a 5 m/s jet the height has to be ≈ 2.5 m and to get a 10 m/s jet the height has to be ≈ 10 m. This initiated the introduction of closed headboxes. In such a headbox the pressure inside is higher than the surrounding atmospheric pressure. In figure 4.4 an example of a modern hydraulic headbox can be found. It basically consists of the manifold (a), tube package (b) and nozzle (c). The manifold is tapered in such a way that the pressure is constant throughout its length. The tube package serves two main purposes. At the up-stream side the open area is low, giving a high-pressure drop and thus improving spanwise uniformity. This is sometimes followed by discrete steps in increase of the open are. These steps are believed to increase the dispersion of fibre flocs by introduction of turbulence in the flow. At the downstream side the open area is maximised to reduce the wakes which forms behind the separating walls. Finally the nozzle is designed to give the desired headbox jet.

4.4. The fibre (pulp) suspension

The idealised fibre suspension consists of a Newtonian liquid with non-buoyant rodlike stiff particles (cylinders). This two-phase fluid is an extension of the case of non-buoyant solid spheres with a diameter d in a liquid solvent. The solid stiff rods introduces two new parameters. These are the aspect ratio of the particles L/d (L is the length) and the volume concentration C_v . The pulp fibre suspension used in paper manufacturing is not at all as well behaved as this idealised suspension.

One feature of most pulp fibre suspensions is the capability to form flocs when diluted in water, so called fibre flocculation. This is a feature closely connected to consistency and fibre properties. Not only is the rheology of such a suspension dependent of its history but also on time.

Mason (1954) discussed the mechanism of fibre flocculation and concluded that it is due to the fibres mechanically bonding to each other. A review can be found by Kerekes *et al.* (1985). It was found that the flocculation starts when the concentration reach a critical value. The presence of fibre flocs is very important for the resulting flow field. One of the main goals when the paper is formed is to avoid the presence of flocs that will otherwise decrease the uniformity of the paper sheet.

The rheology of a fibre suspension is thus extremely complicated. If the flow of a fibre suspension through a pipe is studied three regions of different flow behaviour can be observed. These can be seen in figure 4.5. For low flow velocities the pulp flows as a plug. At the walls of the channel there is a thin layer of almost pure water, which acts as a lubricating layer. In order to get the suspension flowing the initial force/pressure has to exceed a certain threshold limit. This is due to the initial static friction between the fibre network and the channel wall. This is in rheology usually referred to as yield-stress. When the flow rate is increased the shear at the walls cause disruption of the network into flocs and/or fibres close to the walls. This state can be referred to as turbulent, but in order to prevent confusion with turbulence in an ordinary fluid, fluidised is a better word. The fluidisation can be both at floc level and at fibre level. The plug flow is gradually broken up as the velocity is increased. Finally the flow will be completely fluidised.

This does not necessarily mean that turbulence appears in the same manner as for single-phase linear (Newtonian) fluids, where turbulence is characterised by the continuous spectrum of scales in the flow, ranging from the most energetic large scales to the smallest micro scales where energy is dissipated into heat by viscosity. If, the concentration level is increased, non-linear effects start to appear and the 'viscosity' will depend on the flow conditions. Due to the fibres and flocs the available scales are fewer and the spectrum is not continuous. The smallest scales are most probably of the same size as the fibres, since the presence of the fibre will suppress scales in the flow, which are smaller than the fibre size. Fibre flocs will also limit the scales, since the flow within a fibre floc will probably not be turbulent (due to the small velocity difference between the floc and fluid). The dissipation of turbulent kinetic energy within the fibre suspension will also differ from the case of a single-phase fluid. It has been shown that strong agitation of a fibre suspension generates network strength. Hence energy is transferred from the larger scales into the fibre network.

The discussion of the flow in a headbox can be performed using the word turbulence, if one with turbulence imply a non-deterministic, i.e. chaotic, behaviour of the

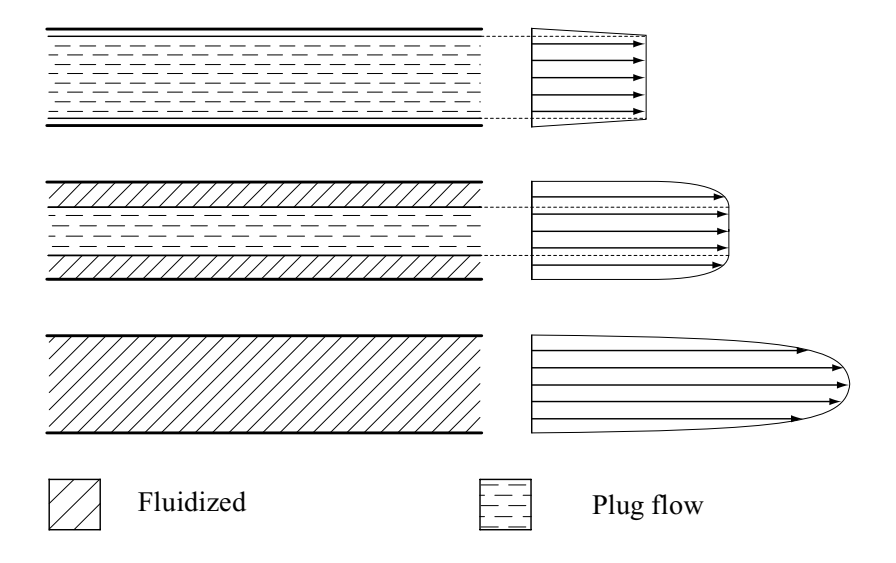


FIGURE 4.5. The different flow regimes for a pulp suspension through a pipe.

fluctuations. Due to the presence of fibres and fibre flocs this turbulence will probably not have the same characteristics as turbulence in a Newtonian liquid. However, at low fibre concentrations the viscosity will still be constant (independent of the flow-field), i.e. the suspension can still be regarded to be a Newtonian fluid, and the viscosity will increase with an increasing concentration level, see e.g. Ralambotiana *et al.* (1997).

A 'true' Reynolds number can not be obtained for a fibre suspension flow. An approximation can of course be made with a suitable apparent viscosity. Such an estimate will give a viscosity of the fibre suspension, which easily is one order of magnitude higher than the viscosity of water. Therefore, results obtained at low Reynolds numbers using Newtonian fluids can also be relevant for flows of fibre suspensions at higher velocities. If, for example, pure water is considered to be the fluid in the paper manufacturing process $Re = \mathcal{O}(10^5)$, but for the model experiments performed by Söderberg & Alfredsson (1998) $Re = \mathcal{O}(10^3)$. The difference in Reynolds number may still be a second order phenomena when compared to the presence of fibres and fibre flocs, which will have a strong influence on the liquid behaviour.

4.5. Cellulose fibres

There are two main types of cellulose fibre: softwood (e.g. spruce or fir) and hardwood (e.g. birch or eucalypt). Softwood fibres are longer, has a higher slenderness, and thus generate more fibre flocs at a given concentration level. Softwood fibres are stronger

but hardwood fibres give a better paper formation. Often mixtures of hardwood and softwood fibres are used in a paper product.

There are two main principles for separating the individual fibres from the wood composite: chemical and mechanical pulping. In chemical pulping the lignin, which glues the fibres together in the wood is chemically dissolved. This leaves the individual cellulose fibres rather intact. In mechanical pulping, the fibres are just separated and the lignin will be left as a cover on the fibres. This will result in stiffer fibres, with a higher flocculation tendency.

CHAPTER 5

Fluid mechanics of headbox flow

Headboxes have been used since the early 19:th century and they have been successively refined. Also, there is a vast amount of different designs. However, the understanding of the physics (mostly fluid mechanics) involved has not reached the same level as the technical knowledge. The design tools have mainly been individual skills and empiricism. Basic hydrodynamic considerations have been made, but these have to some extent been heuristic. A good review is given by Parker (1972).

5.1. Manifold and tube bank

The manifold is usually designed with a tapered, gradually decreasing cross-section, figure 5.1. At the large area end the flow enters and in the small area end there is often an overflow in order to make it possible to control the pressure drop. The open area is usually about 10%. Due to this design, the flow towards the tubes is asymmetric and it is a well known phenomenon that the flow towards a sink (hole) can set up a strong swirl (figure 5.2), especially if there is some imperfection in the flow towards the hole. With the flow rates used in paper manufacturing this can give a considerable effect and create strong vortices in a tube bank.

The geometry is usually such that the holes have sharp edges, which can give rise to flow separation downstream the inlet. This separation can possibly be reduced if the flow is swirling, since this prevents separation. The strong acceleration in the entrance flow to the tubes can possibly contribute to the dispersion of flocs as well as align fibres in the flow direction. The tubes usually have a step-wise increase in area, which will generate turbulence. Hence, the steps will also have an influence on the dispersion on fibre flocs.

If the inlets to the tube bank are circular, the cross-section will usually be transformed to rectangular or even hexagonal, in order to achieve as large open area as possible at the downstream end of the tube bank. This will avoid the formation of large wakes behind the dividing walls. It has been shown that ducts with sharp corners can introduce secondary flows, see e.g. Schlichting (1979).

5.2. Flow conditions in the nozzle

If the discussion is limited to a Newtonian (linear) fluid such as water or air some conclusions regarding the behaviour of the turbulence can be drawn. From these it

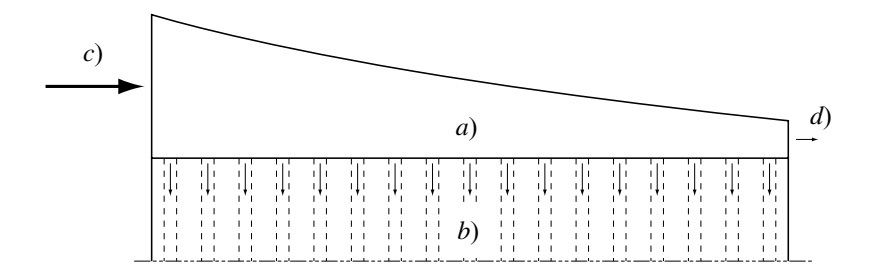


FIGURE 5.1. Manifold and tube bank, (a) manifold, (b) tube bank, (c) inflow and (d) overflow.

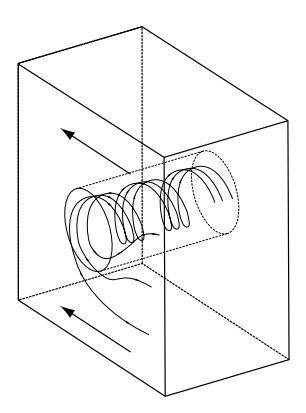


FIGURE 5.2. Swirl created by the asymmetric approach flow to the diffuser tubes

may be possible to obtain a physical insight in what is happening in a converging nozzle. Some of the dominating features may then be transferred to a fibre suspension flow through a headbox.

The absolute level of streamwise fluctuations (turbulence level), u_{rms} , at a specific position in the nozzle is given by

$$u_{rms}^2 = \frac{1}{T} \int_0^T [u'(t) - \overline{u}]^2 dt,$$

and has the dimension [m/s]. Here \overline{u} , is the local mean velocity. Due to the acceleration of the flow in the nozzle the relative turbulence level, u_{rms}/\overline{u} , decreases throughout the nozzle. The absolute turbulence level can however both be decreasing and increasing. An investigation of the turbulence in a plane contraction was

recently presented Parsheh (1999). It was shown that the mean flow can (accurately) be described with laminar flow equations due to the strong relative suppression of the turbulent quantities in the contracting channel. A calculation of the boundary layer in the convergent channel using Pohlhausens boundary layer solution, see Schlichting (1979), showed good agreement with hot-wire measurements in the latter part of the model headbox. It was shown that the boundary layer is turbulent in the beginning of the headbox, but experiences a reversed transition i.e. re-laminarisation, as the flow is accelerating. However, the suppression of turbulent quantities in the equations describing the mean flow still allows spanwise and streamwise mixing, since the absolute fluctuation levels varies only slightly in the core of the channel. The investigation by Parsheh, also made comparisons between the measurements and numerical calculations of the flow using different turbulence models. The flow in the plane contraction is not axisymmetric in the plane perpendicular to the streamwise direction and is accelerating. The results indicate that the tested turbulence models cannot predict the turbulent flow in the channel. The well known K- ϵ model performed poorly, which can be understood since it is based on the assumption of isotropic conditions in the flow. As stated earlier the mean flow-field in the headbox can be estimated accurately neglecting the turbulent dissipation. If the fluid consists of a fibre suspension the presence of fibres will probably dominate the behaviour of the flow.

5.3. Streak size in boundary layers and confined flows

Streamwise aligned elongated structures (vortices or velocity streaks) are common in many different flow situations. Typically the size of those streaks (CD¹ spatial extent), is of the order of the boundary layer thickness or the smallest size of the geometry perpendicular to the flow direction.

In wall bounded flows the origin is usually closely connected to the shear at the solid surfaces. The streaks in these cases normally have a size similar to the thickness of the shear layer. For the case of a boundary layer flow the streaks typically have a size comparable to the boundary layer thickness.

The geometry itself can also be responsible for the size of the streaks, as in the case of vortex stretching in accelerating flows. One example of this would be the flow in a nozzle (headbox), where the final vortex diameter will be of the same size as the slice thickness. For the case of curved and/or rotating flows where centrifugal instabilities are present, e.g. Taylor-Couette or Dean instabilities, the size of the vortices is also determined by the channel thickness.

For the flow situations discussed above, the elongated structures usually covers the spanwise width of the flow as in, for example, velocity streaks in the zero pressure gradient boundary layer flow or vortices in the case of the Dean-type centrifugal instability.

¹MD, CD and ZD are the same as the streamwise, spanwise and normal directions respectively. This notation is common in paper technology and will be used in the following.

5.4. Origin of streaks in headbox flow

As mentioned in the introduction there are several mechanisms which can give rise to streaks in headbox jets and thus in the final sheet. The results presented show some features of a headbox jet.

If boundary layers are assumed to be responsible for streaks, as in the case of transient growth or the Görtler centrifugal instability, it is known from a purely hydrodynamic point of view that the spatial scales of the streaks or vortices are of the same order of magnitude as the boundary layer thickness. This would imply a width of the streaks substantially smaller than the thickness of the jet since the boundary layer is thin at the nozzle exit, see e.g. Lindqvist (1996). This would give streaks which has a size (CD extent) of the order of 1 mm. No such streaks were observed in the visualisations and wavelet evaluation. Also, based on the assumed flow field, see e.g. Söderberg (1994), it seems unlikely that there will be a possibility for the Görtler instability to appear since the radius of curvature points towards the wall.

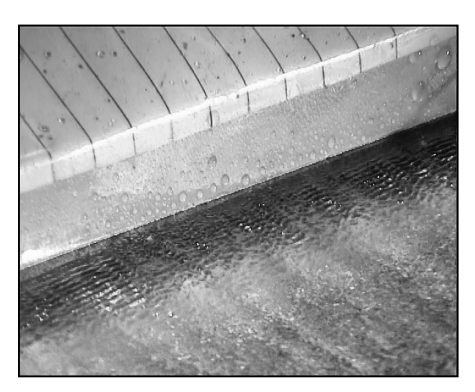
If the fluid is inviscid and irrotational (potential flow), the velocity field at the exit of a nozzle is such that the centrifugal forces could set up a secondary flow similar to what is found in the case of the Dean instability. There are no observations of the instability for this idealised case.

Another possible source for streaks would be the feed structure upstream of the headbox nozzle, which would initiate vortices in the jet by the vortex stretching mechanism. Indications of this was found by Söderberg (1999b). By using a wavelet transform a pattern with a wavelength comparable to the CD size of the feed structure was identified. This pattern could not be found by averaging a series of images, but only by averaging the series of wavelet transforms obtained for each individual image. This implies that these streaks are not stationary, but moves or oscillates in CD.

5.4.1. Waves and break-up in the headbox jet

For the case of a plane water jet it was shown by Söderberg & Alfredsson (1997), that strong MD aligned streaky structures could be created inside the jet. The creation of these streaks in the jet was found to be closely connected to the appearance of waves on the jet surface, which are a consequence of the ZD velocity profile relaxation, see Söderberg & Alfredsson (1998). For the case of the low Reynolds number water jet the water was seeded with iriodin particles, which react on shear gradients in the flow. Hence, there is a possibility to observe what happens inside the jet. Also, the wave breakdown in the low Reynolds number water jet appears in connection with drop formation at the jet surface.

Söderberg (1999b) showed that this type of waves and the related break-up can be found in the flow of a "real" headbox jet. In figure 5.3 an image of the outflow from a headbox nozzle can be seen. The surface of the liquid jet is visible and wave disturbances similar to those in figure 3.8 are clearly present. It is possible that streaks



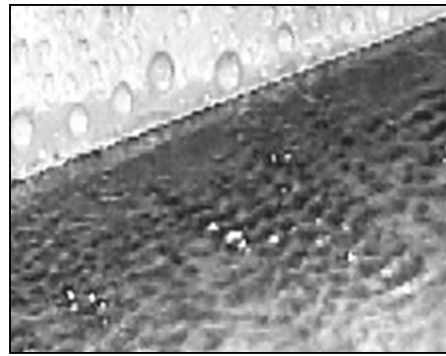


FIGURE 5.3. Jet issuing from a headbox. Nozzle and jet with a visible centimeter scale (left) and a close-up with visible waves (right).

are created inside the headbox jet in the same way as in the case of a low Reynolds number water jet. The drop formation on the surface was clearly visible, but since the fluid was not seeded with iriodin particles there were no means with which the streak creation could be directly observed

The expected size (CD and ZD) of such streaks is not clear. The earlier investigations indicate that streak width is of the same size as the ZD thickness of the jet. But, since the waves are related to the shear field in the jet there is a big difference between the low Reynolds number jet and the headbox jet. For the headbox jet the boundary layers at the exit are only a fraction of the jet thickness and for the low Reynolds number jet the "boundary layers" cover the whole channel thickness, i.e. fully developed Poiseuille flow. Thus, if the waves scale with the boundary layer thickness, the streaks obtained by wave breakdown in the headbox jet would be of the order of 1 mm. However, since the redistribution of momentum and mass in the jet has to take place over the whole jet thickness it is most likely that the streaks created will be present throughout the jet thickness.

One of the main results concerning the low Reynolds number water jet was the localisation of the break-up of the jet to positions where upstream inhomogeneity was stronger. Thus, if there is a higher upstream disturbance level at some position, due to e.g. an irregularity on the walls of the nozzle, the break-up will take place where this disturbance interacts with the waves. This means that the waves (actually the profile relaxation) act as an amplifier to upstream disturbances.

If the waves were not present on the surface of the headbox jet, the situation would be similar to the flow of the low Reynolds number jet with the slit nozzle. For this case streaks can be visualised with the shadowgraph method, see Söderberg (1994). If one looks at the visualisation of the water jet with transmitted light there are only waves present and no MD aligned streaks can be found. The only lines in MD are the phase

shifts of the waves and thus they indicate a presence of velocity differences in the jet. Hence, there seems to be streaks present in the flow.

The waves are not a primary source of streaks, but at a late stage surface roughness induced by the wave breakdown (jet break-up) can give strong effects at the jet/wire impact. Also, the waves themselves could of course give rise to CD variations, a least at the surface of a paper sheet. Even though their spatial size is not large the small-scale formation could deteriorate.

5.5. Influence of suspended fibres

The presence of fibres in the water clearly has an impact on the properties of the flow. However, the results by Söderberg (1999b) show that the waves on the jet surface are more homogeneous in the flow of a fibre suspension jet compared to the flow of a water jet. This could be due to a damping of either upstream disturbances or of the instability development in the free liquid jet. Also, it was found that the strength of the break-up of the jet was lower for the fibre suspension than for the pure water jet at the same flow rate.

CHAPTER 6

Summary of Papers

Paper 1

This paper contains three parts, which are aimed at the flow of a two-dimensional liquid jet leaving a plane channel. The first part is concerned with the laminar steady flow of the jet, which is numerically solved by the method of finite differences using the two-dimensional Navier-Stokes equations. The solution is obtained for the velocity field as well as the location of the free surface. The boundary of the grid in physical space coincides with the free surface, which gives a well defined surface. The results from the numerical computations showed that if the streamwise coordinate, x, is scaled with the Reynolds number, the velocity distributions are similar. This is only valid for high Reynolds numbers (Re > 100). Also, it was found that the distance it takes to relax a given velocity profile at the exit of a finite length channel, is considerably longer than the length of the channel, as long as the flow in the channel is far from fully developed. This was explained by the differences between the boundary conditions at the channel walls and the conditions at the free surface.

The second part is concerned with the temporal linear stability of the calculated velocity profiles. This was investigated by solving the Orr-Sommerfeld equation with appropriate boundary conditions in the liquid and surrounding gas. The solution to this eigenvalue problem was obtained by a spectral method using Chebyshev polynomials. Variations were made in wavenumber and Reynolds number. Also, the effect of a less developed upstream flow in the channel was investigated. The results clearly show the presence of five unstable modes (three sinuous and two dilatational). The two dilatational modes form pairs with two of the three unstable sinuous modes. One of these two pairs is unstable closest to the channel exit, where the velocity profile exhibits strong inflection points. This pair is also unstable over a large range of wavenumbers. The second pair is unstable irrespective of the position in the jet and for lower wavenumbers. The third unstable sinuous mode is unstable in a region bounded in space (streamwise position), Reynolds number and wavenumber.

The third part contains experiments on the basic flow and stability of the jet. These experiments were performed with water, and pitot tube measurements of the velocity profiles in the jet showed good agreement with calculated profiles. Visualisations of the jet flow was also performed with both the shadowgraph method and by

seeding the flow with reflective platelets. For high Reynolds numbers (Re>700) the shadowgraph visualisations showed streamwise travelling waves on the surface of the jet. The waves were homogeneous in the spanwise direction and as Reynolds number was increased the jet experienced a break-up, which seemed to be related to the presence of the waves. The particle visualisation showed that the break-up created strong streamwise streaks in the jet.

In the paper it is also shown that the waves found on the jet could be triggered by acoustic disturbances. By forcing the waves with a loudspeaker the amplitude variation of the disturbance through the thickness of the jet was obtained by hot-film anemometry. Also, when the waves on the jet were forced, the streamwise wavenumber variation were extracted from shadowgraph images. This was compared to results from stability calculations and the agreement was found to be fair.

Paper 2

This paper is focused on the difference in streak-creation between a plane channel nozzle and a slit nozzle, i.e. a two-dimensional *vena contracta*. The paper is experimental and the results are obtained by shadowgraph and particle visualisations. The paper discusses the influence of nozzle design on streaks in the jet. For low Reynolds numbers both jets were smooth and showed no sign of disturbances in the core region. However, when the Reynolds number was increased the channel jet showed waves at the surface, which experienced a break-up. The slit jet did not show any disturbances on the surface for Reynolds number where the channel jet was totally broken up. By the particle visualisation the presence of streaks could be shown. These were found to be originating from upstream disturbances. As the Reynolds number was increased these streaks became more numerous and started to oscillate in the spanwise direction. By the particle visualisation it was also possible to show that this type of streaks also were present in the channel jet. By averaging captured frames it was shown that the positions where streaks, originating from the break-up of the channel jet, were formed corresponded to the presence of streaks originating from within the nozzle.

The disturbance level preceding the channel was also altered and the result was that the break-up at low Reynolds numbers was increased. However, at higher Reynolds numbers the difference in disturbance level did not seem to make any observable difference.

Paper 3

In this paper experiments performed with a headbox from the *EuroFEX*-experimental papermachine, at *STFI*, Stockholm, are presented. The experiments were conducted by visualisations, which were recorded using a High-Speed video camera. This made it possible to follow transient events and individual fibre flocs.

The paper presents visualisations performed with both reflected light and light transmitted through the jet. This is done for flow of pure water as well as a fibre suspension. The digitised images were quantified with the aid of a continuous wavelet transform. This was done in both streamwise and spanwise directions of the jet (MD and CD). The images and the wavelet transform clearly showed the presence of wave disturbances on the headbox jet. Those had a similar behaviour to the waves found in Paper 1 and lead to a break-up, which is similar to what was found in Paper 2. The wavelet evaluation also showed that there were streamwise streaks in the visualisations of the jet. These had a spanwise (CD) extent of the order of the jet thickness, which was 10 mm. A peak in the distribution of the spanwise (CD) wavelet transform were found. This corresponded to a spanwise wavelength of ≈ 30 mm. This was only found if the wavelet results for a series of 50 images were averaged. However, if the average of 50 images were processed with the wavelet transform no peak was found. The peak was explained by the influence of the tube package, which is situated upstream of the nozzle contraction. It was concluded that this could be the result of streamwise vortices which were oscillating in the spanwise direction. Hence, they are not visible in averages of many images.

The high-speed visualisations were used to obtain estimates of the (surface) velocity of the jet. This was done with the PIV technique. The results showed streamwise velocity streaks.

Paper 4

This paper is concerned with the stability of the relaxational plane liquid jet.

Spatial stability calculations were performed in a similar manner as the temporal stability calculations were performed in paper 1. The results are compared to experimental data, which were obtained by quantification of shadowgraph visualisations. In the experiments the jet was subjected to an acoustic disturbance, which induced waves in the jet. The wavenumber and amplitude variation in the images were extracted by a Morlet wavelet transform. The theoretical wavenumber variation was in excellent agreement with the experimental results. This clearly identified the type of mode which the visible waves represent. In order to determine if the observed waves were a result of a sinuous or dilatational disturbance a comparison between the calculated integrated growth and wave amplitude was made. Based on this comparison it was concluded that the visible waves most probably are dilatational. Also, from the stability calculations it is clear that the sinuous mode has a considerably lower integrated growth given the same parameters as in the experiments.

The paper also shows that the relaxational jet can be absolutely unstable. Far downstream in the jet where the velocity profile becomes close to uniform, the results are in agreement with results found in literature. Hence, only the sinuous mode is absolutely unstable far downstream. In the region close to the nozzle it was found that both modes have pinch points, and that the dilatational mode can be dominant. This difference was explained as being the consequence of the velocity profile in the jet. It

was argued that for the profiles in the beginning of the jet the modes behave as though the surfaces are uncoupled.

An explanation for the break-up of the jet was sought by considering the integrated growth of the convective disturbances. This was shown to give a possible explanation to the movement of the break-up line as the Reynolds number is increased.

Paper 5

This paper is aimed to correlate the behaviour of the headbox jet and the final paper sheet, especially the influence of the headbox contraction ratio on. The paper contains visualisations of the headbox jet issuing from a three-ply headbox, where the different layers have been given different colour. This was done in order to correlate the appearence of the jet with paper sheets, which were produced during the trials.

Three different contraction ratios of the headbox nozzle were used in the experiments. The results clearly showed that a low contraction nozzle gives a jet with a very disturbed surface and large transient streaks. For a high contraction ratio nozzle the jet surface only showed small disturbances compared to the low contraction nozzle. For this case fairly stationary streaks were present in the jet, which cause mixing, The medium contraction was shown to give the best result, i.e fewer streaks and lower mixing.

Acknowledgments

Without exaggerating I have to say that without my supervisor Prof. Henrik Alfredsson this thesis would probably never have been written. If it wasn't for his excellent course in compressible flow the idea of becoming a PhD student would never have hit me. His genuine interest and knowledge the field of fluid mechanics has been a strong source of inspiration. I also have to express my gratitude to Prof. Bo Norman, Dept. of Paper technology for introducing me to the field of paper forming. He was also part in the initiation of this project and he has, together with Prof. Fritz Bark, opened up the paper technology business at the Department of Mechanics.

I wish to thank those who have shared office space with me during the years, Dr. Per Elofsson, Dr. Masaharu Matsubara and Lic. Mehran Parsheh, for enjoying discussions regarding everything (actually also fluid mechanics, i.e. fruitful discussions).

I also wish to thank Carl Häggmark for our 07.00 breakfast meetings and Dr. Nils Tillmark for all interesting lunch discussions. Johan Westin is gratefully acknowledged for his participation in preparing this thesis and correcting my blousy englich.

Also, the working conditions has been wonderful in the presence of so many skilled and friendly people, previous and present graduate students of the "Labbet", research assistants, technicians and visiting scientists: Kristian Angele, Dr. Andrey Bakchinov, Doc. Anders Dahlkild, Doc. Barbro Muhammad Klingmann, Dr. Ardeshir Hanifi, Jens Fransson, Johan Gullman-Strand, Marcus Gällstedt, Lic. Bo Johansson, Ulf Landen, Lic. Renaud Lavalley, Björn Lindgren, Fredrik Lundell, Lic. Mikael Sima, Dr. Torbjörn Sjögren, Lic. Mats Ullmar and Jens Österlund.

Lennart Hermansson, STFI is thanked for his help during the experiments at the *EuroFEX* machine

This work has been financially supported by NUTEK, the Swedish National Board for Industrial and Technical Development, and the participating partners within the Faxen Laboratoriet.

Finally, I wish to thank my wife Satu for her love and support and my three daughters Mikaela, Madeleine and Julia for being.

References

- AIDUN, C. K. & KOVACS, A. E. 1995 Hydrodynamics of the forming section The origin of nonuniform fiber orientation. *TAPPI J.* **78** (11), 97–106.
- ALFREDSSON, P. H. & MATSUBARA, M. 1996 Streaky structures in transition. In *Transitional Boundary Layers in Aeronautics* (ed. R. A. W. M. Henkes & J. L. van Ingen), pp. 374–386. Elsiever Science Publishers.
- BARNES, H. A., HUTTON, J. F. & WALTERS, K. 1989 An Introduction to Rheology. Elsevier Science
- BOGY, D. B. 1979 Drop formation in a circular liquid jet. Ann. Rev. Fluid Mech. 11, 207–227.
- Brennen, C. 1970 Cavity surface wave patterns and general appearance. *J. Fluid Mech.* 44, 33–49
- BROWN, D. R. 1961 A study of the behaviour of a thin sheet of moving liquid. *J. Fluid. Mech* **10** (2), 297–305.
- DEBLER, W. & Yu, D. 1988 The break-up of laminar liquid jets. *Proc. Roy. Soc. Lond. A* 415, 106–120.
- DOMBROWSKI, N. & FRASER, R. P. 1954 A photographic investigation into the disintegration of liquid sheets. *Phil. Trans. R. Soc. London Ser. A* 247, 101–131.
- DRAZIN, P. G. & REID, W. H. 1981 Hydrodynamic Stability. Cambridge University Press.
- ELOFSSON, P. A., KAWAKAMI, M. & ALFREDSSON, P. H. 1999 Experiments on the stability of streamwise streaks in plane Poiseuille flow. *Phys. Fluids* **11** (4), 915–930.
- FARGE, M. 1992 Wavelet transforms and their applications to turbulence. *Ann. Rev. Fluid Mech.* **24**, 395–457.
- GOEDDE, E. F. & YUEN, M. C. 1970 Experiments on liquid jet instability. *J. Fluid Mech.* 40, 495–514.
- GOODWIN, R. T. & SCHOWALTER, W. R. 1995 Arbitrarily oriented capillary-viscous planar jets in the presence of gravity. *Phys. Fluids* **7** (5), 954–963.
- HAGERTY, W. W. & SHEA, J. F. 1955 A study of the stability of plane fluid sheets. *J. Appl. Mech.* 22, 509–514.
- HAGLUND, L., NORMAN, B. & WAHREN, D. 1974 Mass-distribution in random sheets Theoretical evaluation and comparison with real sheets. *Sven. Papperstidn.* 77 (10), 362.
- HASHIMOTO, H. & SUZUKI, T. 1991 Experimental and theoretical study of fine interfacial waves on thin liquid sheet. *JSME Int. J.* **34** (3), 277–283.

- HENNINGSON, D. S. & ALFREDSSON, P. H. 1996 Stability and transition. In *Turbulence and Transition Modelling* (ed. M. Hallbäck, D. S. Henningson, A. V. Johansson & P. H. Alfredsson), Kluwer.
- HOYT, J. W. & TAYLOR, J. J. 1977 Waves on water jets. J. Fluid Mech. 83, 119–227.
- JOSEPH, D. D. 1978 Slow motion and viscometric motion; stability and bifurcation of the rest state of a simple fluid. *Arch. Rat. Mech. Anal.* **56**.
- KEREKES, R. J., SOSZYNSKI, R. M. & DOO, P. A. T. 1985 The flocculation of pulp fibres. In 8th Fund. Res. Symp., Oxford (ed. V. Punton). Mech. Eng. Publ. Ltd.
- KLINGMANN, B. G. B., BOIKO, A. V., WESTIN, K. J. A., KOZLOV, V. V. & ALFREDSSON, P. H. 1993 Experiments on the stability of Tollmien-Schlichting waves. *Eur. J. Mech.* B/*Fluids* **12** (4), 493–514.
- LAMB, H. 1932 Hydrodynamics, 6th edn. Dover.
- LI, X. & TANKIN, R. R. 1991 On the temporal stability of a two-dimensional viscous liquid sheet. *J. Fluid Mech.* **226**, 425–443.
- LIENHARD, J. H. 1968 Effects of gravity and surface tension upon liquid jets leaving Poiseuille tubes. *J. Basic Eng.* **226**, 425–443.
- LIN, S. P. 1981 Stability of a viscous liquid curtain. J. Fluid Mech. 104, 111–118.
- LIN, S. P., LIAN, Z. W. & CREIGHTON, B. J. 1990 Absolute and convective instability of a liquid sheet. *J. Fluid Mech.* **220**, 673–689.
- LIN, S. P. & ROBERTS, G. 1981 Waves in a viscous liquid curtain. J. Fluid Mech. 112, 443–458
- LINDQVIST, A. N. 1996 Structures in the flow from paper machine headboxes. *Tech. Rep.*. Lic. Eng. Thesis, Luleå University of Technology.
- MASON, S. G. 1954 Pulp Paper Mag. Can 55 (13), 96.
- MATSSON, O. J. E. & ALFREDSSON, P. H. 1990 Curvature- and rotation-induced instabilities in channel flow. *J. Fluid Mech.* 210, 537–563.
- MATSUBARA, M., ALFREDSSON, P. H. & WESTIN, K. 1998 Boundary layer transition at high levels of free stream turbulence. In *Paper no 98-GT-248 ASME. International Gas Turbine & Aeroengine Congress & Exhibition, Stockholm.*
- MCCARTHY, M. J. & MOLLOY, N. A. 1974 Review of stability of liquid jets and the influence of nozzle design. *Chem. Engng. J.* 7, 1–20.
- NORMAN, B. 1996 Hydrodynamic developments in twin-wire forming An overview. *Paperi ja Puu Paper and Timber* **78** (6–7), 376–381.
- PAI, S. I. 1954 Fluid Dynamics of Jets. Van Nostrand.
- PARKER, J. D. 1972 The sheet forming process. TAPPI PRESS.
- PARSHEH, M. 1999 Aspects of boundary layers, turbulence and mixing in a plane contraction with elastic vanes, envisaging potential application to paper manufacturing. *Tech. Rep.*. Lic. Eng. Thesis, TRITA-MEK TR 1999:4, KTH, Dept. of Mechanics.
- PLATEAU, J. 1873 Statique expérimentale et théorique des liquides soumis aux seules forces moléculaires. Cited by Lord Rayleigh in Theory of Sound, 2nd edn, vol. II., Dover.
- RALAMBOTIANA, T., BLANC, R. & CHAOUCHE, M. 1997 Viscosity scaling in suspensions of non-Brownian rodlike particles. *Phys. Fluids* **9** (12), 3588–3594.
- RAYLEIGH, L. 1896 Theory of Sound, 2nd edn. Dover.

- ROBERTSON, A. A. & MASON, S. G. 1961 Wet end factors affecting the uniformity of paper. In *2nd Fund. Res. Symp., Oxford* (ed. F. Bolam). Tech. Sec. British Paper and Board Makers' Assoc., London.
- SCHLICHTING, H. 1979 Boundary layer theory, 7th edn. McGraw-Hill.
- SÖDERBERG, D. 1994 An experimental study of the stability of plane liquid jets. Master's thesis, Dept. of Mechanics, Royal Institute of Technology.
- SÖDERBERG, L. D. 1997 Experimental and theoretical studies of plane liquid jets. *Tech. Rep.*. Lic. Eng. Thesis, TRITA-MEK TR 1997:1, KTH, Dept. of Mechanics.
- SÖDERBERG, L. D. 1999a Absolute and convective instability of a relaxational plane liquid jet. *To be submitted*.
- SÖDERBERG, L. D. 1999*b* A comparison between the flow from a paper machine headbox and a low Reynolds number water jet. In *Tappi Engineering Conference, Anaheim*.
- SÖDERBERG, L. D. & ALFREDSSON, P. H. 1997 Observation of streaky structures in a plane water jet. In *Tappi Engineering Conference*, *Nashville*.
- SÖDERBERG, L. D. & ALFREDSSON, P. H. 1998 Experimental and theoretical stability investigations of plane liquid jets. *Eur. J. Mech.* B/Fluids 17 (5), 689–737.
- SQUIRE, H. B. 1953 Investigation of the instability of a moving liquid film. *Br. J. Appl. Phys.* **4**, 167–169.
- TAYLOR, G. I. 1959a The dynamics of thin sheets of fluid II. Waves on fluid sheets. *Proc. Roy. Soc. A* 253, 296–312.
- TAYLOR, G. I. 1959b The dynamics of thin sheets of fluid III. Disintegration of fluid sheets. *Proc. Roy. Soc. A* **253**, 313–321.
- TAYLOR, G. I. 1960 Formation of thin flat sheets of water. Proc. Roy. Soc. A 259, 1-77.
- TENG, C. H., LIN, S. P. & CHEN, J. N. 1997 Absolute and convective instability of a viscous liquid curtain in a viscous gas. *J. Fluid Mech.* **332**, 195–120.
- TILLET, J. P. 1968 On the laminar flow in a free jet of liquid at high Reynolds numbers. *J. Fluid Mech.* **32**, 273–292.
- WESTIN, K. J. A., BAKCHINOV, A. A., KOZLOV, V. V. & ALFREDSSON, P. H. 1998 Experiments on localized disturbances in a flat plate boundary layer. Part 1. The receptivity and evolution of a localized free stream disturbance. *Eur. J. Mech. B/Fluids* **17** (6), 823–846.
- WESTIN, K. J. A., BOIKO, A. V., KLINGMANN, B. G. B., KOZLOV, V. V. & ALFREDSSON, P. H. 1994 Experiments in a boundary layer subjected to free-stream turbulence. Part I Boundary layer and structure. *J. Fluid Mech.* **281**, 193–218.
- WRIST, P. E. 1961 Dynamics of sheet formation on the fourdrinier machine. In *2nd Fund. Res. Symp., Oxford.* Tech. Sec. British Paper and Board Makers' Assoc., London.
- YAKUBENKO, P. A. 1997 Capillary instability of an ideal jet of large but finite length. *Eur. J. Mech.* B/Fluids 16 (1), 39–47.
- Yu, T. & Liu, T. 1992 Numerical solution of a newtonian jet emanating from a converging channel. *Computers Fluids* **21** (4), 812–823.

48 REFERENCES